Formation of Diphosphates. A NMR Study on the Mechanism and Stereochemistry of Diphosphate Formation from Chiral Dioxaphosphorinanes

Ron Hulst,*,†,‡,§ Johanna M. Visser,† N. Koen de Vries,|| Robert W. J. Zijlstra,⊥ Huub Kooijman,▽ Wilberth Smeets,▽ Anthony L. Spek,▽,○ and Ben L. Feringa*,⊥

Contribution from the Department of Chemical Analysis, University of Twente, P.O. Box 217, 7500 AE Enschede, The Netherlands, Department of Physical and Computational Chemistry, DSM Research, P.O. Box 18, 6160 MD Geleen, The Netherlands, Department of Organic and Molecular Inorganic Chemistry, University of Groningen, Nijenborgh 4, 9747 AG Groningen, The Netherlands, and Bijvoet Center for Biomolecular Research, Crystal and Structural Chemistry, University of Utrecht, Padualaan 8, 3584 CH Utrecht, The Netherlands

Received August 3, 1999. Revised Manuscript Received January 3, 2000

Abstract: During the use of chiral *2-oxo-1,3,2-dioxaphosphorinanes* as derivatizing reagents in the enantiomeric excess determination of amines, alcohols, and unprotected amino acids, minor traces of side reaction products were observed by ^{1}H and ^{31}P NMR spectroscopy. Analysis of the reaction mixture showed that the side products are in fact *diphosphates* and several *intermediates* leading to their formation. From an analytical, mechanistic, and stereochemical point of view, the study of *unexpected new* reaction intermediates leading to diphosphates is of particular interest. Due to the easy structural modification of the starting materials in both enantiomerically pure and racemic forms as well as easy access to oxygen-labeled materials for complete structural elucidation of both intermediates and diphosphates, we accomplished a complete structural analysis. Also a mechanistic proposal for their formation proved possible using 1D and 2D ^{1}H and ^{31}P NMR techniques as well as the X-ray data of both starting material and two of the products.

Introduction

Although the elucidation of the factors governing substitution reactions at phosphorus is considered highly important for various (*biological*) pathways[1,2] involving the phosphorus nucleus, results have not led to conclusive interpretations with respect to the mechanism of *diphosphate* formation. One of the first reports on the mechanism of diphosphate formation was presented by Simpson and Zwierzak,[3] describing the condensation reaction between *2-chloro-5,5-dimethyl-2-oxo-1,3,2-dioxaphosphorinane* (**1**) and *2-hydroxy-5,5-dimethyl-2-oxo-1,3,2-dioxaphosphorinane* (**2**), leading to diphosphate **3**. Using phosphoric methyl ester **4** with ^{18}O-labeling at the phosphoroxy oxygen in the condensation reaction with chlorophosphorinane **1**, it was established that the labeled oxygen was distributed between the bridged oxygen and one of the phosphoroxy oxygens in diphosphate **3**, although in unequal amounts[4] (Scheme 1).

Two mechanisms were proposed for the formation of **3**, involving initial attack of the oxo (route a) or alkoxy (route b) oxygen. From the distribution of the labeled oxygen in **3** it was concluded that route b provided the largest contribution to the formation of diphosphate **3**. Alternative mechanisms, based upon ring-opening of the phosphorinane ring, were ruled out, since earlier studies showed that 1,3,2-dioxaphosphorinanes are highly reluctant toward ring-opening processes.[5]

Cullis and co-workers[6] reinvestigated the Simpson−Zwierzak experiments, using ^{31}P NMR techniques and ^{18}O-labeled materials, and proposed an alternative mechanism for the formation of diphosphate **3** from ^{18}O-labeled chlorophosphorinane **1** and hydroxyphosphorinane **2**, involving the formation of *dioxadiphosphetanes* **8** and **9**. In the process, Berry pseudorotation (BPR)[7] followed by ring opening and chloride elimination leads to bridge-oxygen-labeled diphosphate **3a**, while "direct" elimination from intermediate **7** results in P═O-labeled diphosphate **3b** (Scheme 2).

It should be noted that more recent work suggested that dioxadiphosphetanes *are not* involved in the formation of

† University of Twente.
‡ E-mail: a.j.r.l.hulst@chem.rug.nl.
§ Present address: BioMaDe Foundation, Nijenborgh 4, 9747 AG Groningen, The Netherlands.
|| DSM Research.
⊥ University of Groningen.
▽ University of Utrecht.
○ Address correspondence pertaining to crystallographic studies to this author. E-mail: a.l.spek@chem.uu.nl.

(1) Hengge, A. C. In *Comprehensive Biological Catalysis*; Sinnott, M., Ed.; Academic Press: San Diego, CA, 1998; Vol. 1, pp 517−542. Perreault, D. M.; Anslyn, E. V. *Angew. Chem., Int. Ed. Engl.* **1997**, *36*, 432. Young, M. J.; Chin, J. *J. Am. Chem. Soc.* **1995**, *117*, 10577. Matsumura, K.; Endo, M.; Komiyama, M. *J. Chem. Soc., Chem. Commun.* **1994**, 2019.

(2) Review series: *Advances in Cyclic Nucleotide Research*; Greengard, P., Robinson, G. A., Sr., Eds.; Raven Press: New York, 1980−1988; Vols. 11−19. Corbridge, D. E. C. *In Phosphorous—An Outline of its Chemistry, Biochemistry and Uses*, 5th ed.; Elsevier: New York, 1995.

(3) Simpson, P.; Zwierzak, A. *J. Chem. Soc., Perkin Trans.* **1975**, *1*, 201.

(4) Zwierzak, A. *Phosphorous* **1972**, *2*, 19. Kosolapoff, G. *Organophosphorous Compounds*; John Wiley: New York, 1950; p 339.

(5) McConnell, R. L.; Coover, H. W. *J. Org. Chem.* **1959**, *24*, 630. Edmundson, R. S. *Tetrahedron* **1965**, *21*, 2379. Edmundson, R. S.; Lambic, A. J. *J. Chem. Soc. (B)* **1967**, 577.

(6) Cullis, P. M.; Kay, P. B.; Trippett, S. *J. Chem. Soc., Chem. Commun.* **1985**, 1329.

(7) Berry, P. S. *J. Chem. Phys.* **1960**, *21*, 2379. Berry, P. S. *J. Chem. Phys.* **1960**, *32*, 933.

10.1021/ja992770k CCC: $19.00
Published on Web 03/16/2000

Scheme 1. Reaction Pathways of ^{18}O-Labeled Phosphoric Ester **4** and Chlorophosphorinane **1** Leading to Diphosphate **3**

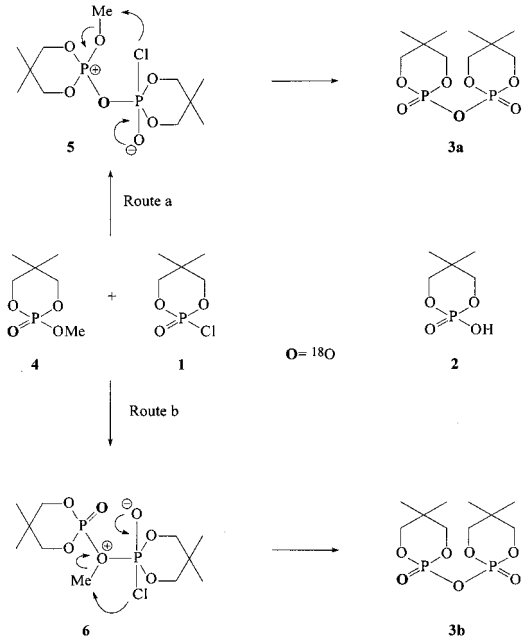

diphosphates, the formation of which is suggested to proceed via a straightforward nucleophilic substitution reaction.[8]

Considering the ambiguities in the mechanisms of diphosphate formation proposed, several problems and questions remain to be addressed: (1) It has not been possible so far to detect the intermediates along the diphosphate pathway(s) directly. (2) It is known that esters of 2-oxo-5,5-dimethyl-1,3,2-dioxaphosphorinanes give rapid chair−chair inversion at room temperature,[9] precluding rigorous stereochemical analysis of the substitution process at the phosphorus center, ruling out the possibility to analyze the stereoselectivity of formation (*axial* vs *equatorial* orientation of the bridged oxygen at both rings in diphosphate **3**). (3) Can additional evidence be obtained for possible competing pathways?

In this paper we report the application of *chiral* chlorophosphorinane **11** in a ^1H and ^{31}P NMR study on the mechanism of diphosphate formation and provide unambiguous evidence for competing pathways and various intermediates involved.

Chlorophosphorinane **11** has been shown to be an excellent derivatizing reagent[10] for the enantiomeric excess determination[11] of chiral alcohols and amines via diastereoselective conversion to the corresponding esters **12** and amides **13**, respectively (Scheme 3). Diphosphate **14** is formed during this reaction as a minor side product.

When compared to the compounds used by Zwierzak and Cullis in diphosphate formation, chlorophosphorinane **11** provides unique possibilities to gain important additional information. The chair−chair inversion, which ruled out the possibility to analyze the stereochemical course of substitution at phosphorus, i.e. equatorial vs axial orientation of the bridging oxygens at both rings in **3**, does not play an important role, since the equatorially oriented phenyl group at the 4-position of the phosphorinane ring system *locks* one chair conformer.[12] The presence of the phenyl group not only leads to a much higher chair−chair inversion energy barrier, but also causes a significant energy difference between both chair conformers. The presence of this stereocenter will also significantly direct the stereochemical coarse of the displacement reaction at the phosphorus nucleus itself.[13,14] Moreover, both stereocenters provide an additional mechanistic tool to obtain information concerning the formation of diphosphate **14**.

Results and Discussion

A. Configuration of Chlorophosphorinanes 11 and 27 and Esters 12 and Amides 13. Since diphosphate **14** is formed as a side product during the derivatization of chlorophosphorinane **11** by alcohols, amines, or amino acids,[10] determination of the configuration and conformation of the esters **12** and amides **13** products is also important for the stereochemical analysis of diphosphate formation.

Besides the configuration and conformation of the substituted phosphorinane ring system, substituents at phosphorus can occupy either an axial or an equatorial position. The stereochemistry of the substituted products and intermediates depends on the initial orientation of the chlorine atom in derivatizing reagent **11** as well as the conformational freedom of the phosphorinane ring system.[2] To establish the absolute configuration at the phosphorus centers after derivatization had taken place, attempts were undertaken to obtain X-ray data on chlorophosphorinane (*R*)-**11**. Unfortunately, the X-ray analysis of (*R*)-**11** did not yield adequate resolution to allow full presentation. The analysis did, however, show both the expected equatorial orientation of the phenyl moiety, locking one chair conformation, and the axial placement of the chlorine atom, observation of which can be explained by the anomeric effect of the 1,3-adjacent oxygen atoms on the chlorine substituent.[15] The influence of the two oxygens lowers the energy contents of the indicated configuration significantly, as confirmed by MNDO[16] and PM3[17] calculations that estimated a ΔE of 8.6 kJ mol^{-1} in favor of the axial orientation of the chlorine substituent. To overcome the resolution problem with (*R*)-**11**, an X-ray analysis was performed on the closely related *o*-chlorine-substituted analogue (*S*)-**27** shown in Scheme 8. The analysis clearly shows the equatorial orientation of the substituted phenyl moiety, whereas the chlorine at phosphorus is axially oriented (Figure 1).

The phosphorinane ring system establishes a *pure* chair conformation as indicated by the puckering parameters $\theta = 15.0(1)°$ and $\Phi = 174.6(5)$.[21] It is assumed that both (*R*)-**11** and

(8) Cullis, P. M.; Kaye, A. D.; Trippett, S. *J. Chem. Soc., Chem. Commun.* **1987**, 1464.

(9) Majoral, J. P.; Bergounhou, C.; Navech, J. *Bull. Soc. Chim. Fr*. **1973**, *11*, 3146.

(10) Hulst, R.; Zijlstra, R. W. J.; Feringa, B. L.; de Vries, N. K.; ten Hoeve, W.; Wynberg, H. *Tetrahedron Lett.* **1993**, *34*, 1339.

(11) For reviews see: Parker, D. *Chem. Rev.* **1991**, *91*, 1441. Hulst, R.; Kellogg, R. M.; Feringa, B. L. *Recl. Trav. Chim. Pays-Bas* **1995**, *114*, 115.

(12) Leusen, F. J. J.; Bruins Slot, H.; Noordik, J. H.; van der Haest, A. D.; Wynberg, H.; Bruggink, A. *Recl. Trav. Chim. Pays-Bas* **1991**, *110*, 13. Zijlstra, R. W. J.; Hulst, R.; de Vries, N. K.; Feringa, B. L. Unpublished results. Hulst, R. *Ph.D. Thesis*, University of Groningen, The Netherlands, 1994.

(13) Gorenstein, D. G.; Powell, R. *J. Am. Chem. Soc*. **1980**, *102*, 6165.

(14) Gordillo, B.; Eliel, E. L. *J. Am. Chem. Soc*. **1991**, *113*, 2172.

(15) White, D. W.; Mc Ewen, G. K.; Bertrand, R. D.; Verkade, J. G. *J. Chem. Soc. B* **1971**, 1454. Bentrude, W. G.; Yee, K. C. *J. Chem. Soc., Chem. Commun*. **1972**, 169.

(16) Dewar, M. J. S.; Thiel, W. *J. Am. Chem. Soc.* **1977**, *99*, 4899.

(17) Stewart, J. P. *J. Comput. Chem.* **1989**, *10*, 209. Stewart, J. P. *J. Comput. Chem.* **1989**, *10*, 221.

(18) Abramczyk, H.; Michailak. *Chem. Phys.* **1988**, *122*, 823.

(19) The introduction of two equatorially oriented methyl groups at the 4- and 6-positions leads, however, to a significantly higher energy barrier for the ring inversion process: Mosbo, J. A.; Verkade, J. G. *J. Am. Chem. Soc*. **1973**, *95*, 204.

(20) It has to be noted that the *S* enantiomer of the chlorophosphorinane **11** is used in the synthesis of the corresponding ester.

(21) Boeyens, J. C. A. *J. Cryst. Mol. Struct*. **1978**, *8*, 317.

Scheme 2. Formation of Diphosphate **3** via Dioxadiphosphetanes **8** and **9**

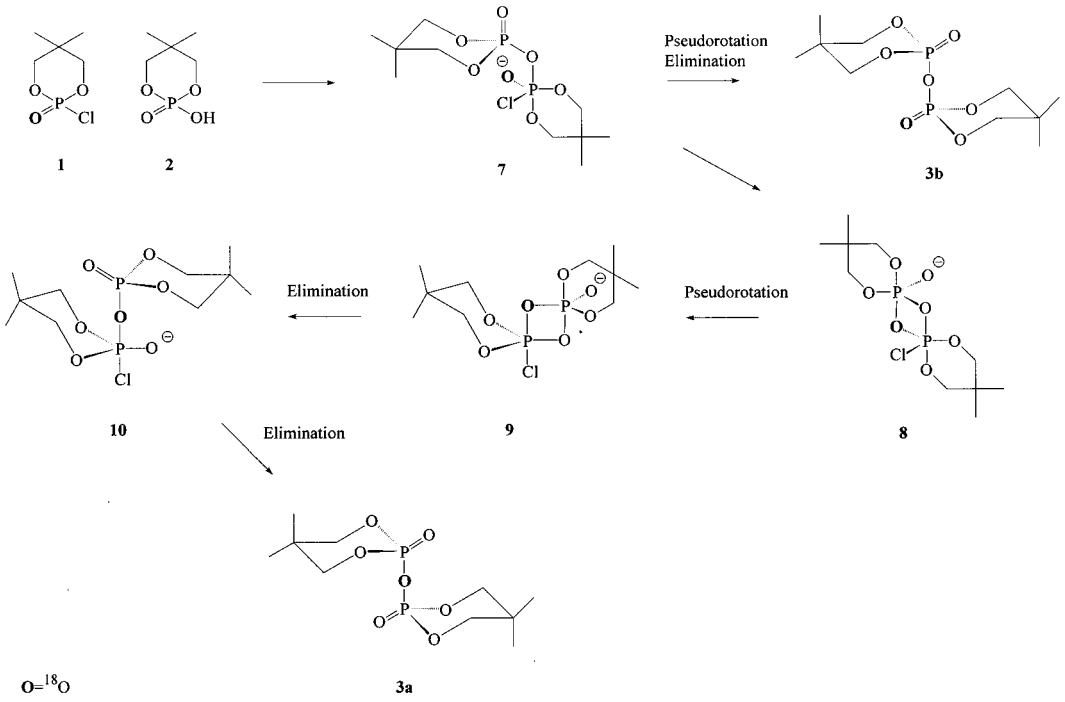

Scheme 3. Chlorophosphorinane **11** and the Product Esters **12**, Amides **13**, and Diphosphate **14** (See the Text for Explanation)

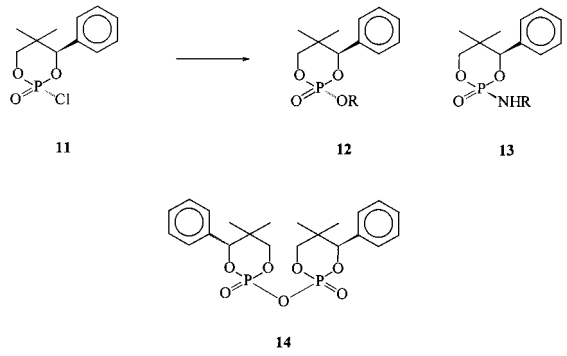

(*S*)-**27** attain the same relative stereochemistry with an equatorial orientation of the phenyl group with regard to the axially placed chlorine at phosphorus, yielding the stereoisomeric products (*R*,*R*)-**11** and (*S*,*R*)-**27**.

Several studies showed that the OR substituents at the phosphorus atom of 2-*OR*-2-oxo-1,3,2-dioxaphosphorinanes, comparable with ester **12**, also show a preference for the axial position, although equilibria exist in solution between the possible chair and twisted boat conformers if the substituents at the phosphorinane ring system are small and the preference for one chair conformer is limited.[18,19] Although MNDO and PM3 calculations showed that for (*S*,*R*)-**12**, where R is (*R*)-2-phenyl-1-propyl, the equatorial orientation of the OR moiety is more stable (ΔE 4.2 kJ mol^{-1}), the differences are small and it is likely that twisted boat conformers do interfere.[9] These results were supported by temperature-dependent ^{1}H NMR measurements with **12** where large shift differences were found for both diastereotopic protons at the CH_2 carbon as a function of the temperature. Also a total collapse of the AB system originating from the diastereotopic CH_2 protons was observed in the phosphorinane ring system at higher temperatures, indicating a large conformational freedom for the phosphorinane ring itself. Unfortunately, from 2D NOESY NMR spectra no conclusive evidence for the orientation of the OR moiety could be obtained. Therefore, an X-ray analysis was carried out on (*S*,*R*)-**12**, where R is (*R*)-2-phenyl-1-propyl (Figure 2).[20]

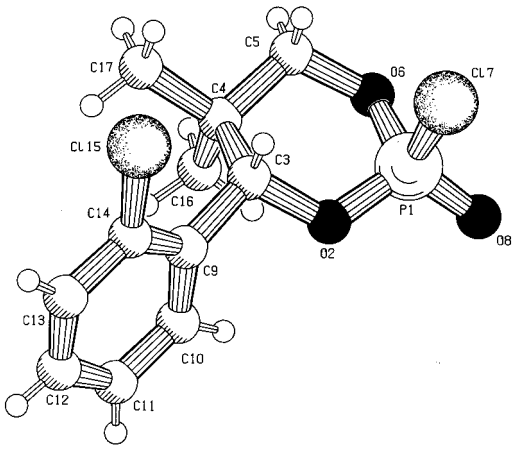

Figure 1. X-ray structure of chlorophosphorinane (*S*)-**27**. Pertinent bond lengths and angles (Å, deg) with su's in parentheses: Cl(7)−P(1) 2.0008(6), O(2)−P(1) 1.5689(11), O(6)−P(1) 1.5673(10), O(8)−P(1) 1.4516(11), Cl(7)−P(1)−O(2) 104.92(4), Cl(7)−P(1)−O(6) 104.55(4), Cl(7)−P(1)−O(8) 112.48(5), O(2)−P(1)−O(6) 106.13(5), O(2)−P(1)−O(8) 114.23(6), O(6)−P(1)−O(8) 113.65(6).

The X-ray analysis shows the phosphorinane ring system to adopt a pure chair conformation (as indicated by the puckering parameters $\theta = 14.3(4)°$ and $\Phi = 198(2)°$)[21] with the phenyl moiety equatorially placed and the ester group axially aligned, indicating that the replacement of the chlorine atom from (*S*)-**11** proceeds with retention of configuration upon reaction with (*R*)-2-phenyl-1-propanol.

Amine substituents are generally accepted to favor the equatorial position.[22] These assumptions are partly based upon the minimized interference of the lone pair electrons situated on nitrogen with the nonbonding electrons of the endocyclic

(22) Bentrude, W. G.; Hargis, J. H. *J. Chem. Soc., Chem. Commun.* **1969**, 1113. Dale, A. J. *Acta Chem. Scand.* **1972**, *26*, 2985.

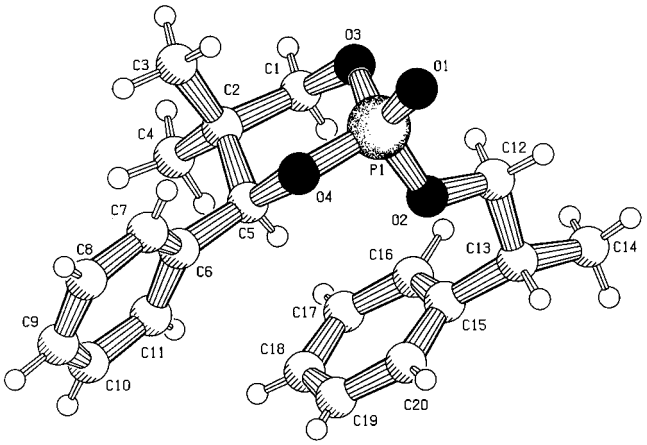

Figure 2. X-ray structure of (*S*,*R*)-**12**, where R is (*R*)-2-phenyl-1-propyl. Pertinent bond lengths and angles (Å, deg) with su's in parentheses: O(1)−P(1) 1.444(4), O(2)−P(1) 1.561(4), O(3)−P(1) 1.571(4), O(4)−P(1) 1.569(4), O(1)−P(1)−O(2) 116.8(2), O(1)−P(1)−O(3) 112.1(2), O(1)−P(1)−O(4) 113.4(2), O(2)−P(1)−O(3) 106.9(2), O(2)−P(1)−O(4) 101.3(2), O(3)−P(1)−O(4) 105.23(19).

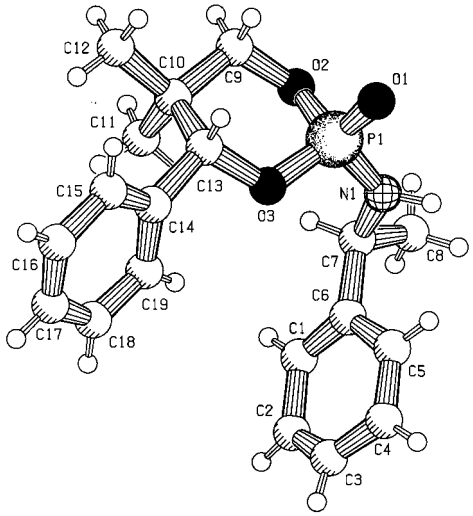

Figure 3. X-ray structure of (*R*,*S*)-**13**, where R is (*S*)-1-phenyl-1-ethyl. Pertinent bond lengths and angles (Å, deg) with su's in parentheses: O(1)−P(1) 1.473(3), O(2)−P(1) 1.577(4), O(3)−P(1) 1.596(3), N(1)−P(1) 1.597(5), O(1)−P(1)−O(2) 113.5(2), O(1)−P(1)−O(3) 114.8(2), O(1)−P(1)−N(1) 113.2(2), O(2)−P(1)−O(3) 101.88(18), O(2)−P(1)−N(1) 106.2(2), O(3)−P(1)−N(1) 106.3(2).

oxygen atoms.[23] Moreover, a *cis*-like orientation of the NH bond toward the phosphoroxy bond is viable, which is also energetically favorable. In contrast to the esters, NMR analysis of (*R*,*S*)-**13**, where R is (*S*)-1-phenyl-1-ethyl, clearly indicated the chair conformation to be present in solution with both the phenyl group and the amine substituent oriented equatorially. These findings were based upon the $^3J_{PH}$ coupling constants of both axial protons in the phosphorinane ring system ($^3J_{PH} \approx 2$ Hz)[24] as well as a strong intramolecular NOE contact between these protons, showing that the phosphorinane ring adopts a chair conformation with the phosphorinane−phenyl group equatorially oriented. Moreover, the benzylic proton at the exocyclic stereogenic center showed an intramolecular NOE contact with the axial methyl group of the phosphorinane system, which is only possible if the amine substituent is oriented equatorially. This assumption was confirmed by an X-ray analysis (Figure 3).

As expected, the phosphorinane ring system establishes a pure chair conformation (as indicated by the puckering parameters $\theta = 177.3(5)°$ and $\Phi = 306(10)°$, with the amine substituent aligned equatorially, (somewhat) distorted toward bisecting (the angle between the P−N bond and the normal of the ring puckering plane amounts to 53°), indicating that the replacement of the chlorine atom from (*R*)-**11** proceeded with inversion of configuration upon reaction with (*S*)-1-phenyl-1-ethylamine. Also the nearly perfect *cis*-type arrangement of the NH−phosphoroxy orientation is clear (dihedral angle 168°).

From these and other data not presented, it is suggested that oxygen nucleophiles react with retention of configuration at the phosphorus nucleus in (*R*)-**11**, whereas amine nucleophiles react with complete inversion. In the esters the OR moiety is oriented axially, allowing great conformational flexibility of the phosphorinane ring system, whereas the amines are aligned exclusively equatorially, resulting in a much more rigid conformation.

B. Formation of Diphosphate (*R*)-14. Although small traces of diphosphate (*R*)-**14** are formed during the derivatization of alcohols, amines, and amino acids using (*R*)-**11**,[10] information upon the exact mechanism of their formation can best be obtained starting from chlorophosphorinane (*R*)-**11** and (if desired) the corresponding hydroxyphosphorinane (*R*)-**15**. The reaction between these compounds leads exclusively to the formation of diphosphate (*R*,*R*)-**14** and intermediates without interference of the esters and amides formed upon derivatization of **11** with alcohols, amines, or amino acids. The intermediates leading to the formation of diphosphate (*R*,*R*)-**14** are, however, completely identical upon the omission of alcohols, amines, and amino acids, although the presence of these materials does clearly influence the rate of formation of both the intermediates and diphosphate (*R*,*R*)-**14**.

Synthesis of Starting Materials. The reactive chlorophosphorinane (*R*)-**11** can be prepared in low yield[25] from hydroxyphosphorinane (*R*)-**15** upon treatment with PCl_5 or from (*R*)-phencydiol (*R*)-**16** after reaction with $POCl_3$ followed by repeated crystallization of the products.[10] Alternatively, (*R*)-**11** can be prepared within a few minutes quantitatively from the readily available hydrogen−phosphorinane (*R*)-**17** after reaction with Et_3N and CCl_4[26−28] (Scheme 4). The last sequence is used unless stated otherwise.

The orientation of the hydrogen atom at the phosphorus nucleus in (*R*)-**17** is proven to be axial, on the basis of NOE interactions between this proton and the (axially oriented) protons at positions 4 and 6 in the phosphorinane ring system (not shown).

Synthesis of hydrogen−phosphorinane (*R*)-**17** using ^{18}O-labeled water yields ^{18}O-labeled (*R*)-**17** and (*R*)-**11** (not shown) with labeling in the phosphoroxy oxygen.[29] The ^{18}O-labeled phosphorinanes proved to be very useful for reaction pathway identification (vide infra).

(23) Bentrude, W. G.; Tan, H. W. *J. Am. Chem. Soc*. **1972**, *94*, 8222.

(24) $^3J_{PH}$ coupling constants for these benzylic protons are 2 Hz typically, whereas the equatorial and axial protons at the 6-position of the dioxaphosphorinane ring have $^3J_{PH}$ coupling constants of 25 Hz for the former and 2 Hz for the latter. This is in agreement with the earlier reported coupling constants for the chair conformation of 2-substituted 5-*tert*-butyl-1,3,2-dioxaphosphorinanes.[22]

(25) Ten Hoeve, W.; Wynberg. *J. Org. Chem.* **1985**, *50*, 4508.

(26) Hulst, R.; Zijlstra, R. W. J.; de Vries, N. K.; Feringa, B. L. *Tetrahedron: Asymmetry* **1994**, *5*, 1701.

(27) Hulst, R.; de Vries, N. K.; Feringa, B. L. *Angew. Chem., Int. Ed. Engl.* **1992**, *31*, 1092. Hulst, R.; de Vries, N. K.; Feringa, B. L. *Tetrahedron* **1994**, *50*, 11721.

(28) This procedure was first described in general by Atherton, F. R.; Openshaw, H. T.; Todd, A. R. *J. Chem. Soc.* **1945**, 660.

(29) This procedure can also be used to determine the ^{18}O contents of ^{18}O target water using ^{31}P NMR techniques: Hulst, R.; Feringa, B. L.; Siertsema, H. K.; Franssen, E. J. F.; Visser, G. M.; Vaalburg, W. *Appl. Radiat. Isot.* **1994**, *10*, 1049.

Scheme 4. Synthesis of Chlorophosphorinane and Hydrogen−Phosphorinane (*R*)-**11** and (*R*)-**17**

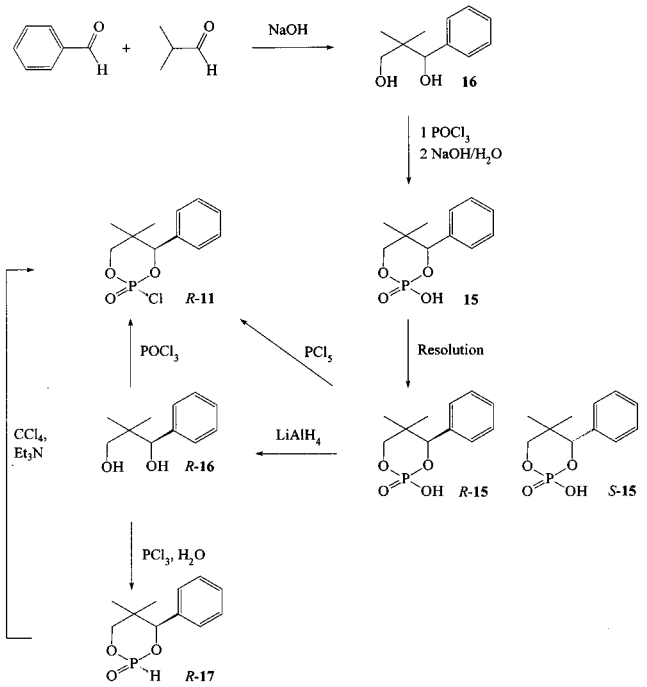

Possible Pathways for the Formation of Diphosphate (*R,R*)-14. The formation of diphosphate (*R,R*)-**14** from (*R*)-phencyphos chlorophosphorinane (*R*)-**11** appears to be sensitive to several factors. The addition of a catalytic amount of the corresponding hydroxyphosphorinane (*R*)-**15** leads to a rate enhancement of the formation of (*R,R*)-**14**. Also, when water is not vigorously excluded, formation of (*R,R*)-**14** is more rapid compared to the reaction under perfectly dry conditions. Since the processes showed complex dependencies on several other factors such as solvent, concentration, and temperature, the discussion will focus on the *qualitative* analysis of the formation of diphosphate (*R,R*)-**14**.

The attack of deprotonated hydroxyphosphorinane (*R*)-**15** at chlorophosphorinane (*R*)-**11** is assumed to proceed in the same manner as the addition of other oxygen nucleophiles, resulting in the formation of a five-coordinated phosphorus (P^V) intermediate.[30,31] Commonly, P^V structures have trigonal bipyramidal geometry (TBP),[32,33] although distortions toward a square-pyramidal (SP) geometry have also been reported.[34] In the trigonal bipyramid, the two axially oriented ligands have slightly longer and weaker bonds than the three equatorial ligands, resulting in different chemical behavior. The differences can be explained in terms of hybridization; phosphorus has pd-hybridization along the *z*-axis and sp^2-hybridization in the equatorial plane. According to the theory introduced by Westheimer,[32] nucleophiles attacking the phosphorinane substrate initially occupy an axial site in the P^V trigonal bipyramid. Furthermore, it is always an axially oriented ligand that is expelled upon conversion of the P^V system to the phosphate stage. P^V-TBP systems show a highly fluctional behavior, usually designated as pseudorotation (BPR, Berry Pseudo-Rotation),[7] in which the five ligands are rapidly distributed over the five sites in the trigonal bipyramid. In this process, two equatorial and two axial ligands interchange their positions via an intermediate SP structure, whereas one (equatorial) ligand, the *pivot*, retains its position.

Ramirez and Ugi[35] have proposed an alternative mechanism, the so-called Turnstile Rotation (TR). In this mechanism, two equatorial ligands move toward each other in the equatorial plane until the angle has become 90°. The third equatorial ligand and one axial ligand are moved by about 9° followed by an internal rotation of the ligands 3 and 4 and of the three ligands 1, 2, and 5. The results of the BPR and TR are exactly the same. Calculations, however, have shown that the transition state for TR is about 2−6 times higher in energy compared to the BPR. Therefore, BPR is the most plausible ligand exchange mechanism in phosphorinanes, and the TR is not taken further into consideration during the following discussion.

The possible modes of addition of (*R*)-**15** to (*R*)-**11** are shown in Scheme 5. The nucleophile, in this case the deprotonated hydroxyphosphorinane (RO^-) (*R*)-**15** enters the P^V-TBP at one axial site, inducing an axial cleavage of the leaving group.[36] It is generally accepted that negatively charged oxygens can adopt only equatorial sites in the P^V-TBP[37] and that pseudorotation can occur prior to the actual bond breaking, placing the proper leaving groups in an axial position. In this way, the nucleophile can approach from four different sites, although the attack of RO^- on the phosphorus atom opposite the P═O bond is not taken into consideration because the P^V-TBP formed will possess a negatively charged oxygen in an axial position, which is energetically unfavorable.

In path 1, the attack of the nucleophile takes place opposite the P−Cl bond; the dioxaphosphorinane formed in this way spans diequatorially (**18**), which is regarded as being energetically unfavorable.[38] Subsequent elimination of chloride results in the formation of diphosphate $\mathbf{14^{ax-eq}}$ which is formed with inversion of configuration with respect to the phosphorus nucleus in the former chlorophosphorinane part of the molecule. This leads to an axial−equatorial orientation[39] of the bridging oxygen with respect to the phosphorus atoms as shown in $\mathbf{14^{ax-eq}}$.

Attack of RO^- opposite the P−O_3 bond (path 2), resulting in P^V-TBP intermediate **19**, gives by cleavage of the axial P−O_1 bond the acyclic phosphorinane diester **23**, which is formed with inversion of configuration with regard to the phosphorus center. Pseudorotation of the P^V-TBP intermediate **19** leads to the formation of another P^V-TBP intermediate **20** and to acyclic **24** or the cyclic product $\mathbf{14^{eq-eq}}$. Both products are formed with retention of configuration at phosphorus. In diphosphate **14**, formed via this route, the bridging oxygen adopts an axial−axial orientation.

(30) For a review concerning phosphorous stereochemistry, see: Hall, C. R.; Inch, T. D. *Tetrahedron* **1980**, *36*, 2059.

(31) Lemmen, P.; Baumgartner, R.; Ugi, I.; Ramirez, F. *Chemica Scr.* **1988**, *28*, 451.

(32) Gorenstein, D.; Westheimer, F. *J. Am. Chem. Soc.* **1967**, *89*, 2762. Westheimer, F. *Acc. Chem. Res.* **1968**, *1*, 70. Kluger, R.; Covitz, F.; Dennis, E.; Williams, L. D.; Westheimer, F. *J. Am. Chem. Soc.* **1969**, *91*, 6066.

(33) Mislow, K. *Acc. Chem. Res.* **1970**, *3*, 321.

(34) Lukenbach, R. *Dynamic Stereochemistry of Pentacoordinated Phosphorous and Related Elements*; Thieme: Stuttgart, 1973.

(35) Ugi, I.; Marquarding, D.; Klusacek, H.; Gokel, G.; Gillespie, P. *Angew. Chem.* **1970**, *82*, 741. Ramirez, F.; Pfohl, S.; Tsolis, E. A.; Pilot, J. F.; Smith, C. P.; Ugi, I.; Marquarding, D.; Gillespie, P.; Hoffmann, P. *Phosphorous* **1971**, *1*, 1.

(36) Gorenstein, D. G.; Powell, R.; Findlay, J. *J. Am. Chem. Soc.* **1980**, *102*, 5077. van Ool, P. J. J. M.; Buck, H. M. *Eur. J. Biochem.* **1982**, *121*, 329.

(37) Holmes, R. R. *Pentacoordinated Phosphorous*; ACS Mongraph No. 175; American Chemical Society: Washington, DC, 1980; Vols. I and II, p 176.

(38) Yu, J. H.; Day, R. O.; Howe, L.; Holmes, R. R. *Inorg. Chem.* **1991**, *30*, 3132. Yu, J. H.; Sopchik, A. E.; Arif, A. M.; Bentrude, W. G. *J. Org. Chem.* **1990**, *55*, 3444. Yu, J. H.; Arif, A. M.; Bentrude, W. G. *J. Am. Chem. Soc.* **1990**, *112*, 7451. Day, R. O.; Kumara Swamy, K. C.; Fairchild, L.; Holmes, J. M.; Holmes, R. R. *J. Am. Chem. Soc.* **1991**, *113*, 1627.

(39) The equatorial or axial description refers to the orientation of the P═O moiety.

Scheme 5. Possible Pathways for the Nucleophilic Attack of Hydroxyphosphorinane (*R*)-**15** at Chlorophosphorinane (*R*)-**11** (See the Text for Explanation)

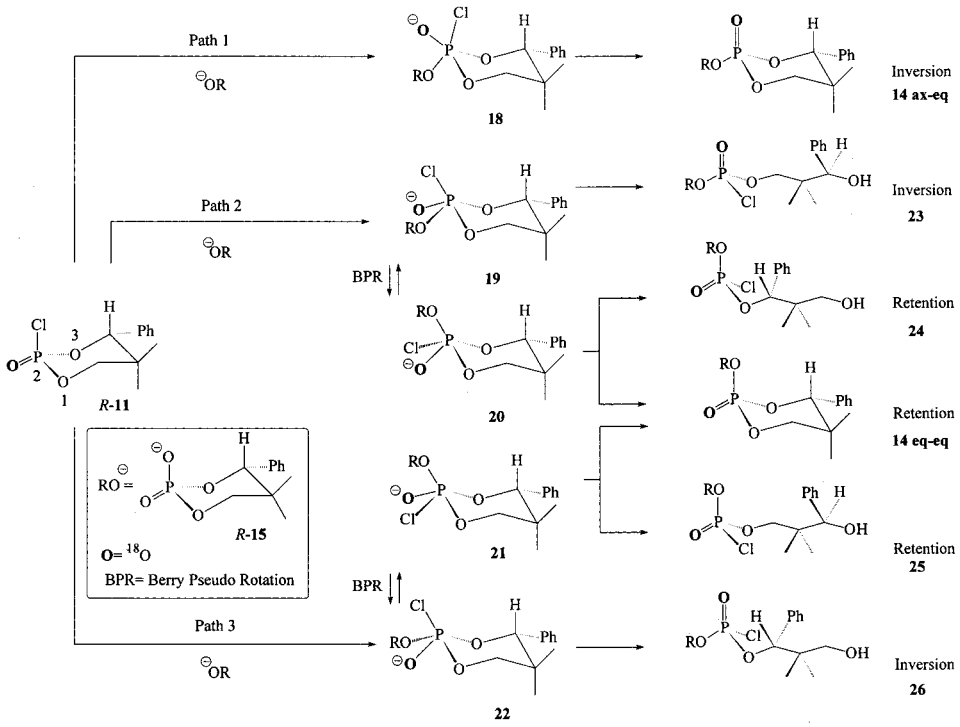

In path 3 attack of RO^- takes place opposite the $P-O_1$ bond. The chloride leaving group is placed equatorially in the P^V-TBP intermediate **22** and can only be eliminated after pseudorotation to **21**, placing the chloride substituent in the axial position. Subsequent cleavage of the axial P−Cl or $P-O_3$ bond leads to the formation of the cyclic diphosphate $\mathbf{14}^{\mathbf{eq-eq}}$ or to the acyclic phosphorinane ester **25**, respectively. Both reactions proceed with retention of configuration at the phosphorus atom. Alternatively, direct cleavages of the axially oriented $P-O_1$ bond in **22** leads to the formation of the acyclic phosphonate ester **26** with inversion of configuration.[39]

Although not all routes are energetically favorable, the results described by, e.g., Buck and co-workers,[40] using analogous systems and oxygen nucleophiles, showed that all products mentioned could in principle be formed though unequally distributed.

Formation of Diphosphate (*R*,*R*)-14 from Phosphorinanes (*R*)-11 and (*R*)-15. Using (*R*)-**11**, in situ derived from (*R*)-**17**,[26] and (*R*)-**15** (both 1.0 mmol), 0.1 mL of Et_3N, and CCl_4 dissolved in $CDCl_3$ (2 mL) or C_6D_6, the formation of diphosphate (*R*,*R*)-**14** is easily monitored by means of ^{31}P NMR spectroscopy (Figure 4).

A total of three signals, two doublets, and a singlet, other than the signals belonging to the starting materials, are initially observed by means of ^{31}P NMR spectroscopy. The presence of these products was also observed by means of ^1H NMR spectroscopy, although the spectra appeared to be very complex due to extensive coupling and signal overlap. The pairs of signals at δ −16.29 and −22.20 ppm, showing an AB type of coupling ($^2J_{PP}$ = 33.0 Hz), are assigned to an intermediate with one of the structures **18**−**22** (Scheme 5). The disappearance of this pair of signals leads to an increase in intensity of the signal

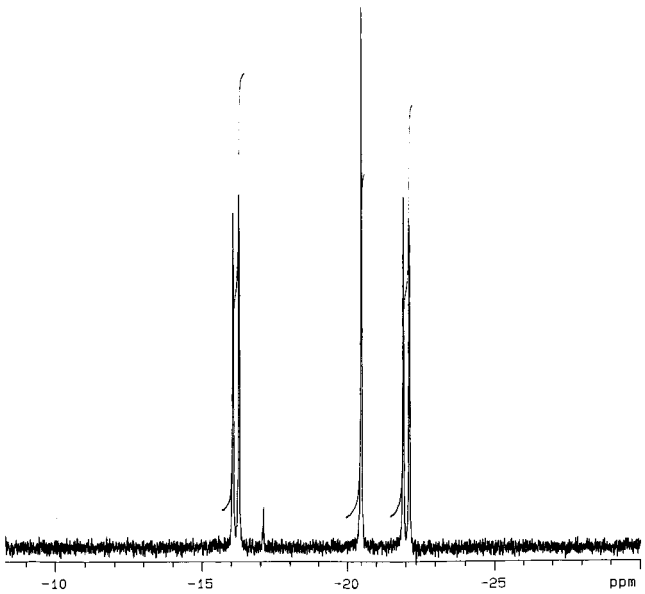

Figure 4. Decoupled ^{31}P NMR spectrum of the reaction mixture during the conversion of (*R*)-**11** and (*R*)-**15** into diphosphate (*R*,*R*)-**14** recorded after 30 min, $CDCl_3$, [L] = 0.01.

located at δ −20.56 ppm, which is assigned to (*R*,*R*)-**14** by comparison with an independently prepared sample (vide infra).[5] The reaction showed a large temperature and solvent dependency and is completed between 1 h at 65 °C and 12 h at 30 °C, both in C_6D_6. The only product is the symmetrical diphosphate (*R*,*R*)-**14**; possible ring-opened products **23**, **24**, **25**, and **26** were not observed.

Especially from the decoupled ^{31}P NMR spectra, it is obvious that the formation of (*R*,*R*)-**14** proceeds diastereospecifically at the phosphorus center; otherwise, a total of four signals, two doublets and two singlets, would be expected. The C_2-symmetrical axial−axial coupled product $\mathbf{14}^{\mathbf{eq-eq}}$ yields only one ^{31}P NMR resonance, the equatorial−equatorial coupled product

(40) Broeders, N. L. H. L.; Koole, L. H.; Buck, H. M. *J. Am. Chem. Soc*. **1990**, *112*, 7475. Broeders, N. L. H. L.; van der Heiden, A. P.; Peeters, I.; Janssen, H. M.; Koole, L. H. *J. Am. Chem. Soc*. **1992**, *114*, 9624. Broeders, N. L. H. L. Ph.D. Thesis, University of Eindhoven, The Netherlands, 1993.

Scheme 6. Possible Diastereomers of Diphosphate (*R,R*)-**14**

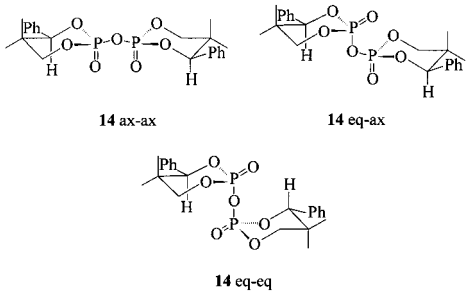

14^{ax-ax} also yields one resonance, and the axial−equatorial bridged diphosphate **14**$^{ax-eq}$ would give two resonances with different chemical shifts and a $^2J_{PP}$ AB coupling.[41] Scheme 6 shows the three possible diastereomeric products (*R,R*)-**14**.

The stereogenic benzylic center in the phosphorinane ring provides an additional source of information concerning the diastereoselectivity, since the formation of diphosphate **14** from racemic starting material would lead to the formation of diastereomers, two *meso* compounds and a *d,l* pair, provided the coupling reaction is stereospecific with regard to phosphorus as shown above. Therefore, diphosphate **14** would give two signals in the decoupled ^{31}P NMR spectrum due to the (*R,R*)- and (*S,S*)-diphosphates (both being symmetrical, giving one signal only) and the *R,S* and *S,R* diastereomers (also symmetrical, yielding one signal). However, when the reaction is not stereospecific with regard to phosphorus, the diphosphate can be formed with a total of 12 different configurations (6 pairs). A *d,l* or *meso* pair with an equatorially oriented P═O in both ring systems, a *d,l* or *meso* pair with both P═O groups axially oriented, and a *d,l* or *meso* pair with one P═O equatorially and one P═O group axially positioned.[39]

By using racemic **11** and **15**, all of the ^{31}P NMR signals previously observed are only doubled, which can be explained by the formation of the *d,l* and *meso* isomers of both the intermediate and diphosphate **14** (Figure 5).

The signals at δ −16.29 and −22.20 ppm, which show an AB coupling ($^2J_{PP}$ = 33.0 Hz), belong to the *RS* form of the intermediate and lead to the formation of (*R,R*)-**14** or (*S,S*)-**14** resonating at δ −20.56 ppm when the progress of diphosphate formation is monitored (Table 1). The *meso* form of the intermediate gives rise to signals at δ −16.44 and −22.32 ppm ($^2J_{PP}$ = 27.8 Hz) and results in the formation of *meso*-**14** resonating at δ −20.62 ppm. The isomers of the intermediate are cleanly and quantitatively converted into (*R,R*)-**14**, (*S,S*)-**14**, and *meso*-**14**.

Since diphosphate **14** gives only one ^{31}P NMR resonance when enantiomerically pure **11** and **15** are used and only two resonances when using racemic **11** and **15**, it can be concluded that the formation of diphosphate **14** is stereospecific at the phosphorus center. Moreover, 2D NOESY NMR and ^{31}P NMR data clearly showed product **14** to be the axial−axial coupled diphosphate **14**$^{eq-eq}$.[39] This also indicates that the observed intermediate is **19** or **22**, since intermediates **20** and **21** possess a chloride leaving group in the axial position that is unlikely to be observed due to the low stability. In the current situation, however, the attack of the deprotonated (*R*)-**15** on chlorophosphorinane (*R*)-**11** is envisioned to occur via the less hindered face of (*R*)-**11**, which is opposite the P−O_3 bond. Therefore, attack according to path 2 (Scheme 5) yielding **19** as the first intermediate is proposed to be the pathway followed, excluding intermediate **22**.

Formation of Diphosphate 14 Derived from Starting Materials Obtained from Different Sources. At this point, both mechanisms proposed by Cullis[6] provide acceptable and reasonably straightforward explanations for the observations made. Less easily understood, however, is the observation that **14** is formed quantitatively when only a catalytic amount or even no hydroxyphosphorinane **15** is available. The involvement of (traces) crystal water could clearly explain these findings, although chlorophosphorinane **11** is shown to be highly reluctant toward straight hydrolysis.[25] To establish a solid explanation, several experiments were conducted using combinations of racemic and enantiomerically pure **11** and **15**.

As indicated, the formation of free hydroxyphosphorinane **15** from chlorophosphorinane **11** is not likely to take place. If hydrolysis is, however, of importance, the reaction between 1 equiv of (*R*)-**11** and 0.5 equiv of (*S*)-**15** to form diphosphate **14** should provide important information. Hydrolysis of (*R*)-**11** to (*R*)-**15** leads to the formation of both (*R,S*)-**14**, from (*S*)-**15** and (*R*)-**11**, and (*R,R*)-**14**, formed from (*R*)-**11** hydrolyzed into (*R*)-**15** and (*R*)-**11**, both in products and intermediates. Both the *meso* form and the *d,l* pair of diphosphate **14** are formed as observed in the ^{31}P NMR spectra, although not all (*R*)-**11** has reacted after 24 h of reaction time at 50 °C in C_6D_6. These results suggest the interference of (traces of) crystal water in the reaction medium, although the exact role remains unclear at the moment.

Next, the conversion of (*R*)-**11** was followed with chlorophosphorinane obtained from different sources. It makes a considerable difference whether (*R*)-**11** is prepared from (*R*)-**17** or from hydroxyphosphorinane (*R*)-**15**. In the former case, only limited conversion to (*R,R*)-**14** takes place. In the latter case nearly all chlorophosphorinane (*R*)-**11** is converted into (*R,R*)-**14**. This can be explained by small traces of (*R*)-**15** (still) present in (*R*)-**11**, which initiates the formation of (*R,R*)-**14**. These observations imply that not (*R*)-**11** but the formed diphosphate (*R,R*)-**14** is subsequently hydrolyzed, yielding 2 equiv of free hydroxyphosphorinane (*R*)-**15**. This indicates that a catalytic amount of free hydroxyphosphorinane, combined with traces of (*crystal*) water, affects the complete conversion of chlorophosphorinane (*R*)-**11** into diphosphate (*R,R*)-**14**.

If, however, a mixture of (*R*)-**15** and (*S*)-**17** was used, diphosphate **14** was formed with an initially (vide infra) observed *d,l:meso* ratio close to 1:1, which cannot solely be explained by simple (*partial*) hydrolysis of (*S*)-**11**, formed from (*S*)-**17**, since this would lead to a 2:1 ratio in favor of the *meso*-**14**, assuming hydrolysis to proceed without (*stereo*)selectivity and no competitive reactions to occur.

Four explanations are possible to account for these observations. Straight hydrolysis of (*R*)-**11** into (*R*)-**15**, which leads to both (*R*)-**15** and (*S*)-**15**, is the first possibility. Second, reaction of 1 equiv of (*R,S*)-**14** with 1 equiv of anion (*S*)-**15** would lead to the formation of 0.5 equiv of (*R,S*)-**14** and of (*S,S*)-**14** with the release of 0.5 equiv of (*R*)-**15** and 0.5 equiv of (*S*)-**15**. After reaction with (*R*)-**11** still present, both *meso*- and *d,l*-**14** are newly formed. A third mechanism would be the attack of liberated chloride ion at (*R,S*)-**14**, yielding (*R*)-**15** and (*S*)-**15** as well as (*R*)-**11** and (*S*)-**11** if the nucleophilic attack proceeds without stereoselectivity. After recombination, *meso*- and *d,l*-**14** are formed again. Unfortunately, reaction of, e.g., (*S*)-**11**,

(41) Gorenstein, D. G. *Phosphorous-31 NMR Principles and Applications*; Academic Press: New York, 1984. Verkade, J. G.; Quinn, L. D. *Phosphorous-31 spectroscopy in Stereochemical Analysis*; VCH Publishers: Deerfield Beach, FL, 1987.Cullis, P. M. In *Phosphorous-31 NMR Spectral Properties in Compound Characterisation and Structural Analysis*; Quin, L. D., Verkade, J. G., Eds.; VCH: Weinheim, New York, and Cambridge, 1994.

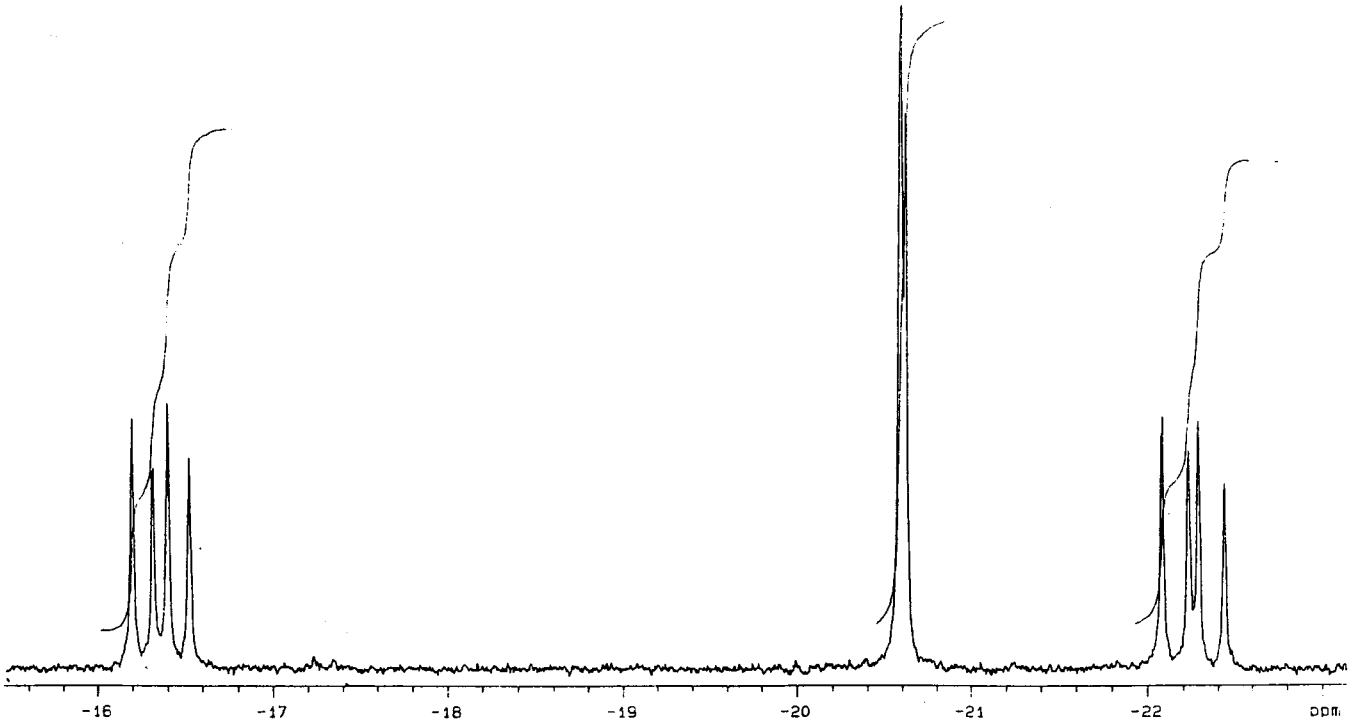

Figure 5. Decoupled ^{31}P NMR spectrum of the reaction mixture during the conversion of (*R,S*)-**11** and (*R,S*)-**15** into diphosphate **14** recorded after 30 min, $CDCl_3$, [L] = 0.01 M.

Table 1. ^{31}P NMR Chemical Shifts and Coupling Constants for Intermediates and Products in the Formation of (Racemic) Diphosphate **14**

compd	δ (^{31}P NMR) (ppm)	δ (^{31}P NMR) (ppm)	J_{PP} (Hz)
(*R,R*)-**14**	−20.56		
(*S,S*)-**14**			
meso-**14**	−20.62		
(*R,R*)-**19**	−16.29	−22.20	33.0
(*S,S*)-**19**			
meso-**19**	−16.44	−22.32	27.8

with (*S*)-**15** yields (*S,S*)-**14**, which is the enantiomer of (*R,R*)-**14** and cannot be distinguished by means of NMR techniques. The most reasonable explanation (the fourth), however, is the direct *hydrolysis of diphosphate* (*R,S*)-**14**. This leads to the formation of both enantiomers of the hydroxyphosphorinane anion **15**, which accounts for the formation of both *meso*- and *d,l*-**14** after subsequent reaction of both enantiomers of **15**. After formation, (*R,R*)-**14** may also hydrolyze, leading to the formation of 2 equiv of (*R*)-**15**. If this should be the case, excess water and base would lead to the formation of hydroxyphosphorinane anion **15** from hydrolysis of diphosphate **14** after chlorophosphorinane **11** has reacted. This is exactly what is found in the experiments carried out under not completely dry conditions. Therefore, the explanation by Cullis and co-workers[6] for the complete scrambling of labeled oxygen over all exocyclic oxygens of the diphosphate formed in the reaction of the phosphorinane methyl ester **4** with the chlorophosphorinane **1** (vide supra) is not necessarily completely correct.

When a small amount of diphosphate is hydrolyzed, there is no need for the proposed attack of the phosphorinane anion on the diphosphate to provide the exchange of labeled and unlabeled material. In this case, the observation of the complete scrambling of labeled and unlabeled oxygen does not exclude the mechanism proposed by Zwierzak.[3,4]

Oxygen-Labeling in the Formation of Diphosphates 14. The presence of P-^{18}O induces a small upfield shift in the ^{31}P NMR resonance frequency of phosphates (ca. 0.02 ppm for each P−^{18}O bond), the magnitude of which is related to the P−O bond order.[42] Cullis and co-workers[6,8] used oxygen-labeling to follow the scrambling process of the oxygens in the formation of diphosphates. In their system, a P−^{18}O single bond produces an upfield shift of 0.023 ppm in the ^{31}P NMR spectrum and a P−^{18}O double bond results in a shift of 0.035 ppm; the effects are additive.

The use of oxygen-labeled (*R*)-**17** and hence (*R*)-**11**, and unlabeled (*R*)-**15**, could provide us with information about the oxygen scrambling and, subsequently, the mechanism of this reaction. Oxygen-labeled (*R*)-**17** was readily prepared following the normal synthetic route,[26] using $H_2{}^{18}O$ (85% labeling degree) to perform the Arbuzov rearrangement. Hydrogen−phosphorinane (*R*)-**17** with 85% labeled and 15% unlabeled oxygen was obtained[29] which showed in the decoupled ^{31}P NMR spectrum two distinguishable signals with a $\Delta\delta$ of 0.034 ppm.

The reaction of ^{18}O-labeled (*R*)-**17** with (*R*)-**15** (both 1.0 mmol), Et_3N (0.1 mL), and CCl_4 (0.1 mL) in C_6D_6 (2.0 mL) at 30 °C yields (*R,R*)-**14** with extensively, though not completely, scrambled labeling of the oxygens.

A total of six signals is observed in the ^{31}P NMR spectrum of **14**, which accounts for the formation of all possible combinations of unlabeled and ^{18}O-labeled diphosphate **14**, as is depicted in Scheme 7.

It has to be noted that the symmetrical diphosphates **14a**, **14c**, **14d**, and **14f** give one signal in the ^{1}H-decoupled ^{31}P NMR spectrum, whereas the unsymmetrically labeled molecules **14b** and **14e** show an extreme AB system, leading to one apparent resonance.[41] The ^{31}P NMR chemical shift difference for these types of labeled molecules is typically comparable to the coupling constant $^2J_{PP}$, giving rise to three resonances instead

(42) Cohn, M.; Hu, M. *Proc. Natl. Sci. U.S.A.* **1978**, *1*, 200. Lowe, G.; Potter, B. V. L.; Sproat, B. S.; Hull, W. E. *J. Chem. Soc., Chem. Commun.* **1979**, 733. Tsai, M.-D. *Biochemistry* **1979**, *8*, 1468. Marschner, T. M.; Reynolds, M. A.; Oppenheimer, N. J.; Kenyon, G. L. *J. Chem. Soc., Chem. Commun.* **1983**, 1289.

Scheme 7. Possible Scrambled Combinations of ^{18}O-Labeled **14** (Other Substituents at Phosphorus Are Omitted for Clarity)

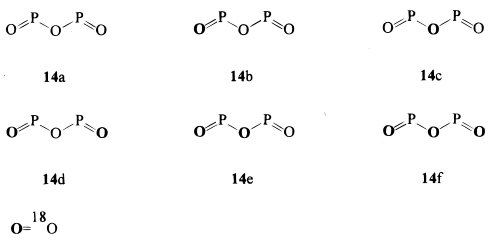

of four. An *extreme* AB system under these conditions gives rise to the observation of only one signal in the ^{31}P NMR spectrum (Figure 6).

As expected, the main product (40%) resembles mono-P═O-labeled diphosphate **14b**, which is formed from labeled (*R*)-**17** and unlabeled (*R*)-**15** (δ −20.60 ppm). Bis-P═O-labeled diphosphate **14d** and the P═O- and P−O-labeled diphosphate **14e** are also formed in reasonable amounts (25% and 20%, respectively), whereas the other three diphosphates, **14a**, **14c**, and **14f**, are formed in small amounts (<5%). Another interesting observation emerges from the ^{31}P NMR spectrum as shown in Figure 6. Because of an incomplete degree of labeling (85% labeled **17** was converted into 85% labeled **11**), it can be concluded that the doublet at δ −16.32 ppm, which is assigned to intermediate **19** as discussed previously (Scheme 5), arises from the phosphorus atom bearing the chlorine substituent. These signals show in the *initial stages* of the reaction the 85:15 labeling ratio that was present in the starting hydrogen−phosphorinane **17**. The other doublet, at δ −22.20 ppm, belongs to the other part of intermediate **19** originating from unlabeled **15**. The labeled and unlabeled intermediate **19** both show the same $^2J_{PP}$ coupling of 33.0 Hz. As the reaction proceeds, intermediates containing one or more scrambled oxygens are formed, in accordance with observations made by Cullis and co-workers for closely analogous systems.[6,8]

C. Use of Substituted Hydroxyphosphorinanes and Chlorophosphorinanes in the Formation of Diphosphates. Although the experiments described above provide us with a rich source of information, several questions remain unanswered. For example, upon reaction of (*R*)-**11** with (*S*)-**15**, it is not completely clear whether anion (*R*)-**15** is formed by hydrolysis of (*R*,*S*)-**14** into 2 equiv of phosphorinane anion **15** (*R* and *S* forms) or (*R*,*S*)-**14** is attacked by a phosphorinane anion (*S*)-**15**, liberating (*S*)-**15** or (*R*)-**15**. Also, chloride attack on (*R*,*S*)-**14** or hydrolysis of (*R*)-**11** can possibly lead to the observed phenomena. An experiment using two slightly modified phosphorus reagents, **27** and **28** (Scheme 8), should provide us with the desired experimental data.[25]

When chlorophosphorinane (*R*)-**27** is allowed to react with (*R*)-**15** (both 1.0 mmol) and Et_3N (0.1 mL) in $CDCl_3$ (2.0 mL) at 30 °C, the ^{31}P NMR spectrum clearly indicates the formation of the "mixed" diphosphate (*R*,*R*)-**32** (Scheme 9).

Diphosphate (*R*,*R*)-**32** gives two doublets at δ −20.37 and −20.84 ppm, with a $^2J_{PP}$ coupling of 23.2 Hz. Furthermore, diphosphates (*R*,*R*)-**14** (δ −20.55 ppm) and (*R*,*R*)-**33** (δ −21.19 ppm) are also observed (Figure 7 and Scheme 9). The formation of the three diphosphates mentioned can be explained by either of the four proposed mechanisms (vide supra).

The observation, however, that *four* different intermediates are formed during the course of the reaction, leading to the formation of *three* different diphosphates (Figures 7 and 8), is unique, and offers the possibility to investigate this reaction at the level of the intermediates themselves. In contrast to the 1D ^{31}P NMR data that do not allow identification of all the resonances because of low resolution, conclusive evidence is obtained from the 2D ^{31}P COSY NMR spectrum,[43] as is shown in Figure 8.

The four different intermediates, for which we propose "general" structures **19**, **29**, **30**, and **31**, are given in Scheme 9. Mixed intermediate **29**, yielding signals in the ^{31}P NMR spectrum situated at δ −16.70 and −22.76 ppm ($^2J_{PP}$ = 29.9 Hz), is formed by the reaction of chlorophosphorinane (*R*)-**27** with hydroxyphosphorinane (*R*)-**15** and leads to the formation of mixed diphosphate **32**.

Knowing, however, that the signals situated around δ −16 to −17 ppm belong to the chloride-substituted part of the intermediates **19**, **29**, **30**, and **31**, it is obvious that, at some stage in the reaction leading to the diphosphates **14**, **32**, and **33**, chlorophosphorinane (*R*)-**11** is also formed. More likely, chloride attack at **32** could also give chloride-substituted (*R*)-**11** as shown for (*R*)-**29**.

The other intermediates can be assigned as follows: intermediate **19** gives signals at δ −16.29 and −22.20 ppm ($^2J_{PP}$ = 33.0 Hz); intermediate **30** yields signals at δ −16.40 and −22.58 ppm ($^2J_{PP}$ = 27.0 Hz). The signals belonging to intermediate **31** are located at δ −17.02 and −22.17 ppm, showing a $^2J_{PP}$ coupling of 27.7 Hz. These assignments were made on the basis of the corresponding coupling constants and integration of the resonances that belong to a single isomer group as well as the correlations obtained from the 2D ^{31}P COSY spectra. The results are collected in Table 2.

Moreover, experiments using (*R*)-**11** and (*R*)-**27** in initial stages showed the groups of signals as discussed belonging to the four intermediates, as well as (*R*,*R*)-**14**, (*R*,*R*)-**32**, and (*R*,*R*)-**33**.

Furthermore, the three diphosphates formed are converted after some time (about 24 h) into the symmetrical *homomorphous* diphosphates **14** and **33**, observation of which demonstrated a large preference of the cyclic phosphoric acid[44] units for the identical counter units (Scheme 9, Figure 7). Results obtained from diffusion (DOSY)[45] and HRMAS solid-state NMR[46] studies also indicate a large preference for identical counter units in both the solution and solid states.

The only acceptable explanation for this observation is based on the assumption that the initially formed diphosphate (*R*,*R*)-**32** is attacked by the liberated chloride ion, yielding either chlorophosphorinane (*R*)-**11** or (*R*)-**27**, or hydroxyphosphorinanes (*R*)-**15** and (*R*)-**28**. It should be noted that diphosphate (*R*,*R*)-**32** can also be attacked by anion (*R*)-**15**, directly yielding diphosphate (*R*,*R*)-**14**, whereas diphosphate (*R*,*R*)-**33** is formed after attack of the liberated anion (*R*)-**28** on the corresponding chlorophosphorinane (*R*)-**27**.

(43) Colquhoun, I. J.; McFarlane, W. *J. Chem. Soc., Chem. Commun.* **1982**, 484.

(44) NMR-based evidence for the conglomerate-like behavior of the corresponding diastereomeric ephedra-based salts was obtained only after cumbersome analysis: Hulst, R.; Kruizinga, W.; Wynberg, H.; Feringa, B. L.; Kellogg, R. M. *Recl. Trav. Chim. Pays-Bas* **1995**, *114*, 220.

(45) The reported phenomena are also extracted from the initial differences in diffusion behavior found for homo- and heteroclusters of the racemic hydroxyphosphorinanes and the corresponding diastereomeric ephedra-based salts: Hulst, R.; Stamps, J.; Ottink, B.; Visser, J. M. Manuscript in preparation.

(46) *Conglomerate-like* behavior is also observed in the ^1H, ^{13}C, and ^{31}P HRMAS solid-state NMR spectra of the materials recorded in both pure solids and slurried materials. Doubling of all the frequencies in the NMR spectra mentioned is due to the different packing in the crystal lattice of the enantiomerically pure and racemic forms: Hulst, R., Visser, J. M. Submitted to *Tetrahedron: Asymmetry*.

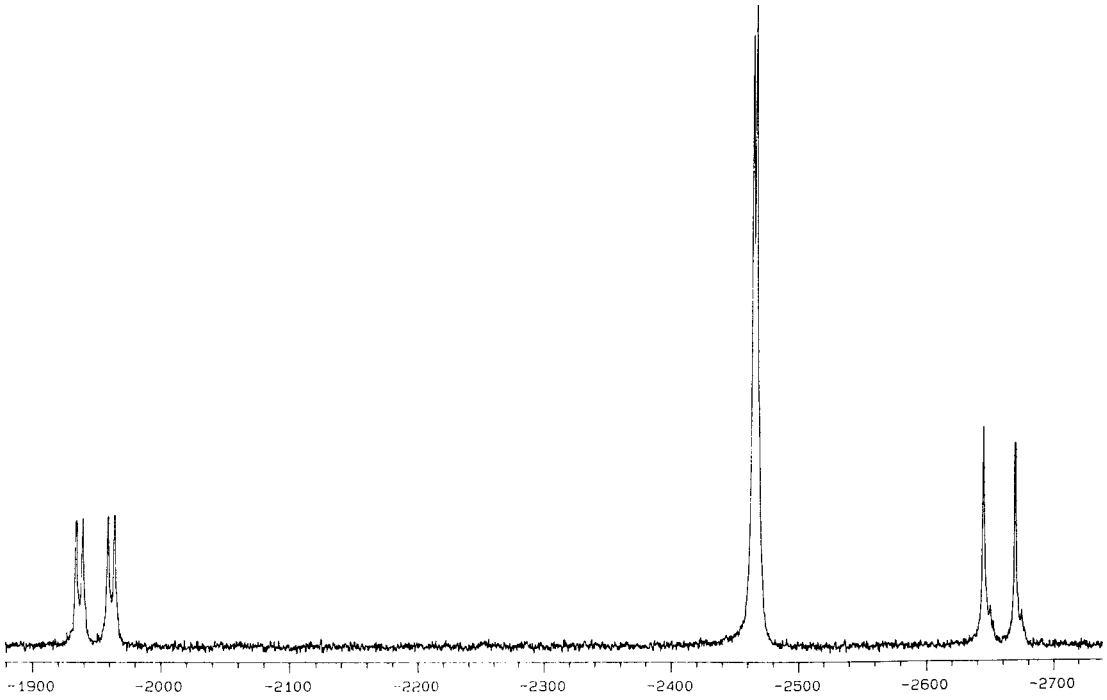

Figure 6. Decoupled ^{31}P NMR spectra of the formation of ^{18}O-labeled (*R,R*)-**14** and intermediates leading to it, recorded in $CDCl_3$, [L] = 0.01 M, 30 °C (axis in hertz).

Scheme 8. Modified Reagents **27**, **28**, and Hydroxyphosphorinane **15** Used for "Mixed Experiments" (See the Text for Explanation)

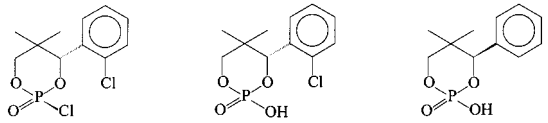

27 **28** **15**

The observation that the chloride ion acts as a nucleophile attacking the diphosphate (*R,R*)-**32** is not accounted for by Zwierzak[3,4] or Cullis,[6,8] although it provides an explanation for the scrambling of the labeled oxygens without the need for the formation of dioxadiphosphetanes **8** and **9**. At this point it is not clear whether one of the three earlier discussed mechanisms are also operating, or the proposed attack of the chloride ion actually is the major route followed.

D. Use of 2D ^{31}P COSY Techniques in the Elucidation of the Formation of Diphosphates. During the course of the research described, it became obvious that the rate of the reaction of (*R*)-**11** and (*R*)-**15** yielding (*R,R*)-**14** showed a large temperature dependence. Normally, reactions were performed at 30 °C. However, experiments carried out using (*R*)-**11** and (*R*)-**15** at temperatures between 45 and 50 °C showed an even more complex behavior than expected on the basis of previous ^{31}P NMR analyses, as is shown in Figure 9. It needs to be emphasized that the (only) final product, however, is diphosphate (*R,R*)-**14**.

The 1D spectrum shows clearly the signals of intermediate **19**, at δ −16.29 and −22.20 ppm ($^2J_{PP}$ = 33.0 Hz), and (*R,R*)-**14** (δ −20.6 ppm). Besides these resonances, several resonances are observed that show extensive phosphorus coupling, which is a strong indication that these intermediates contain more than one, nonequivalent phosphorus atom, connected with each other through a bridging oxygen atom, resulting in the *geminal* phosphorus−phosphorus coupling patterns observed.[47] The other signals, all showing nearly the same coupling patterns, are less easily assigned by the use of 1D ^{1}H and ^{31}P NMR techniques, although the integration is of great help for the full assessment of the 2D ^{31}P COSY spectrum shown in Figure 10.

Scheme 9. Intermediates and Diphosphates Formed in the Reaction of (*R*)-**27** and (*R*)-**15** (See the Text for Explanation)

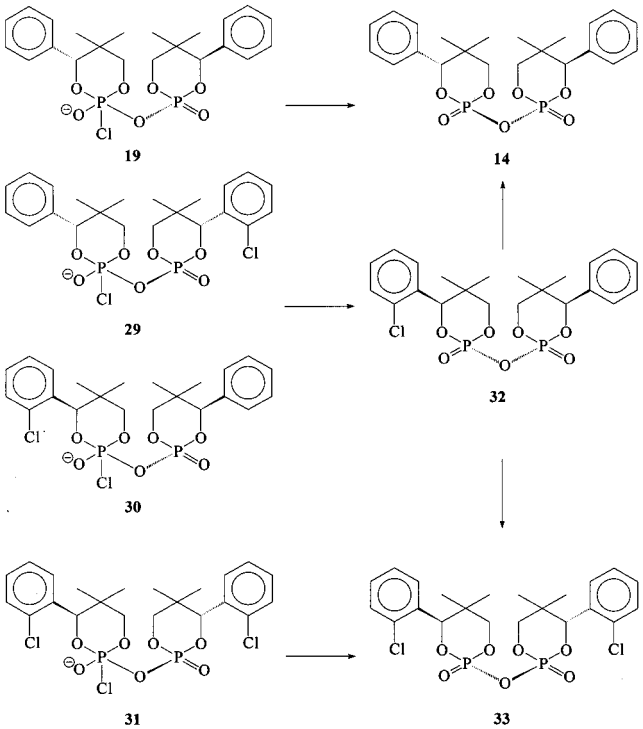

19 **14** **29** **32** **30** **31** **33**

(47) The signal at δ −17.23 ppm (singlet), which is observed regardless of the nature of the hydroxyphosphorinanes used, cannot be assigned unambiguously. It is likely that small amounts of degraded (poly)-phosphorous components give rise to this absorption.

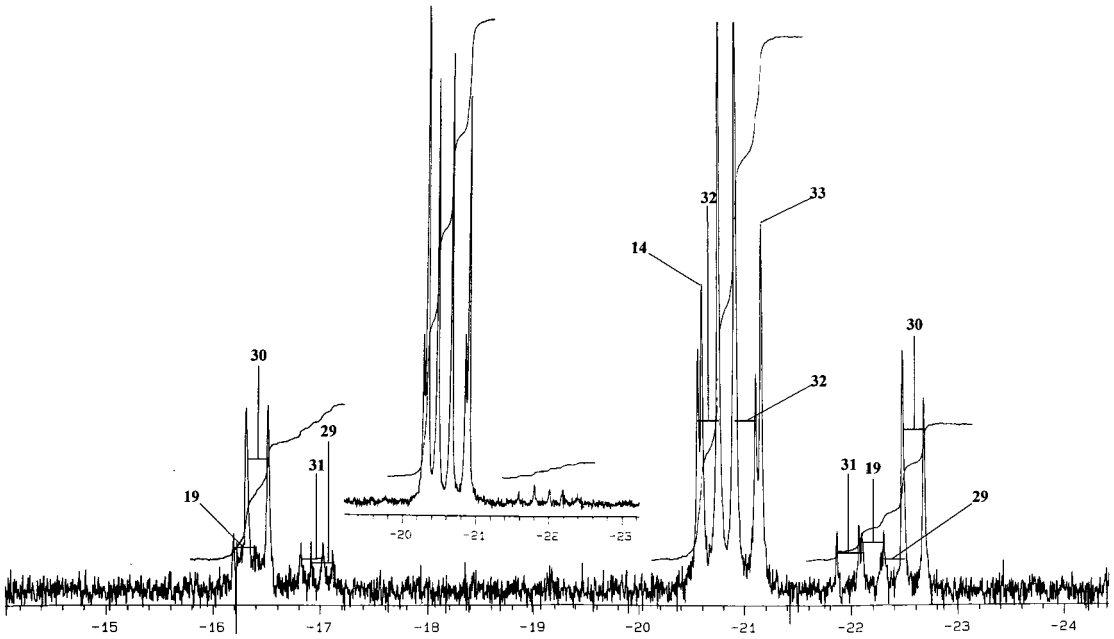

Figure 7. Decoupled ^{31}P NMR spectrum of the reaction products of (*R*)-**27** and (*R*)-**15** after 1 and 24 h (inset), recorded in $CDCl_3$.

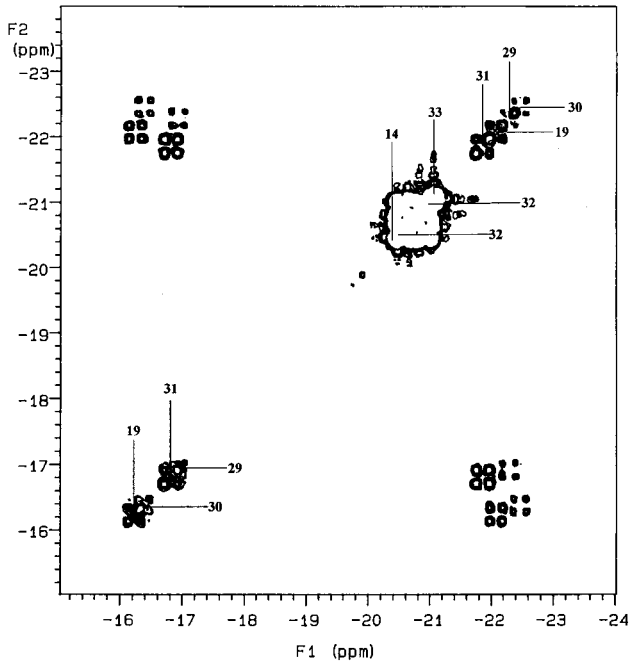

Figure 8. ^{31}P COSY spectrum of the reaction products of (*R*)-**27** and (*R*)-**15**, recorded after 1 h at 30 °C, recording temperature −30 °C, $CDCl_3$.

Table 2. ^{31}P NMR Chemical Shifts and Coupling Constants of Intermediates Leading to the Formation of Mixed Diphosphates (*R,R*)-**14**, (*R,R*)-**32**, and (*R,R*)-**33**

compd	δ (^{31}P NMR) (ppm)	δ (^{31}P NMR) (ppm)	J_{PP} (Hz)
14	−20.56		
19	−16.29	−22.20	33.0
32	−20.37	−20.84	23.2
33	−21.19		
29	−16.40	−22.58	27.0
30	−16.70	−22.76	29.9
31	−17.02	−22.17	27.7

The recording of the 2D ^{31}P COSY spectrum, concerning the intermediates of a still developing reaction, appeared to be rather troublesome, due to the larger time interval needed to record 2D spectra. The intermediates were allowed to build up at 47.5 °C in C_6D_6 as solvent. When they had developed adequately, on the basis of the 1D ^{31}P NMR spectral data, the temperature was quickly brought to −50 °C. This temperature allowed us to record a 2D COSY spectrum, without observable progression of the reaction (only a small amount of $CDCl_3$ had to be added to the reaction mixture to prevent freezing). The experiments were performed using unlabeled as well as labeled materials to obtain maximum information from the experiments. The results as obtained are collected in Table 3.

The phosphorus nuclei leading to the doublet signals at δ −11.43 and −13.73 ppm are clearly correlated, yielding a $^2J_{PP}$ coupling of 18.2 Hz, and are attributed to intermediate **34** (Scheme 10). Although there is no *direct* evidence for this assignment, the observed chemical shifts as well as the fact that both signals at δ −11.43 and −13.73 ppm double when partially oxygen labeled (*R*)-**11** is used in this reaction provide strong indications that this must be a dioxadiphosphetane intermediate.[48] The labeled oxygen is "shared" by the two phosphorus atoms.

The same is found for the signals at δ −11.68 and −18.22 ppm ($^2J_{PP}$ = 21.0 Hz). These also arise from two *O*-connected phosphorus atoms. The labeling experiment, as described above, shows that both signals double upon the use of ^{18}O-labeled starting material (*R*)-**11**. This indicates that the labeled oxygen is again bridged between the two different phosphorus atoms. On the basis of these observations and chemical shifts, the signals are believed to belong to intermediate **35**. The breakdown of **35** yields bridged ^{18}O-labeled intermediate **36**, although this intermediate was not observed as intermediate **36** contains a chlorine leaving group in the axial position. Probably, the elimination of this chlorine is too fast to allow direct detection of intermediate **36** by NMR techniques. So far, the Cullis[6] model provides an acceptable and unambiguous explanation for this part of the observations. That the situation is more complex, however, is indicated by the appearance of two more sets of resonances.

(48) Vedejs, E.; Peterson, M. J. *Top. Stereochem.* **1994**, *21*, 1. Clayden, J.; Warren, S. *Angew. Chem., Int. Ed. Engl.* **1996**, *35*, 241. Hulst, R.; van Basten, A.; Fitzpatrick, K.; Kellogg, R. M. *J. Chem. Soc., Perkin Trans. 1* **1995**, 2961.

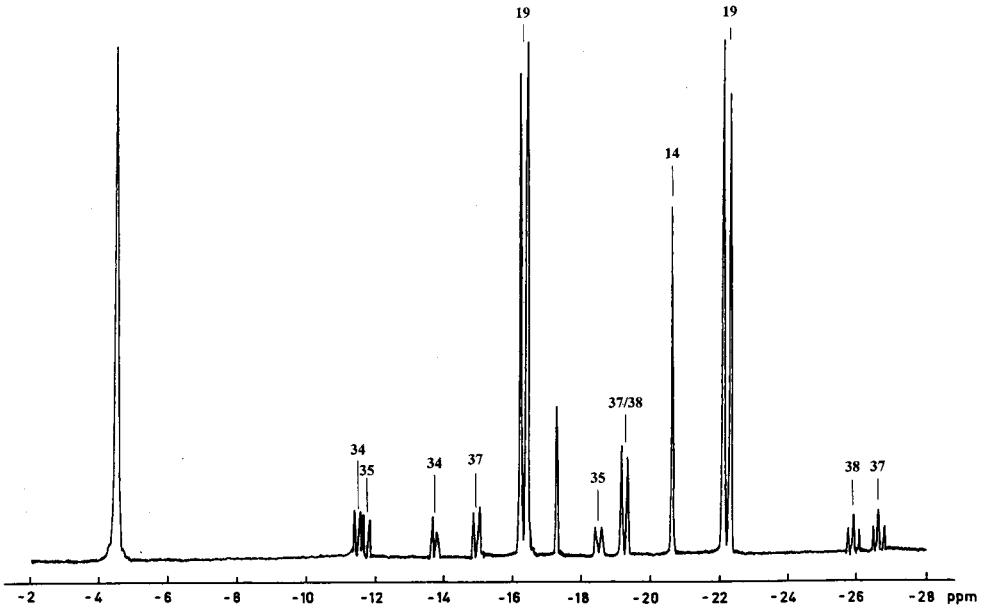

Figure 9. ^{31}P NMR spectrum during the formation of (*R,R*)-**14** from (*R*)-**11** and (*R*)-**15** at 47.5 °C, recorded at −50 °C, solvent $CDCl_3/C_6D_6$, [L] = 0.01 M.

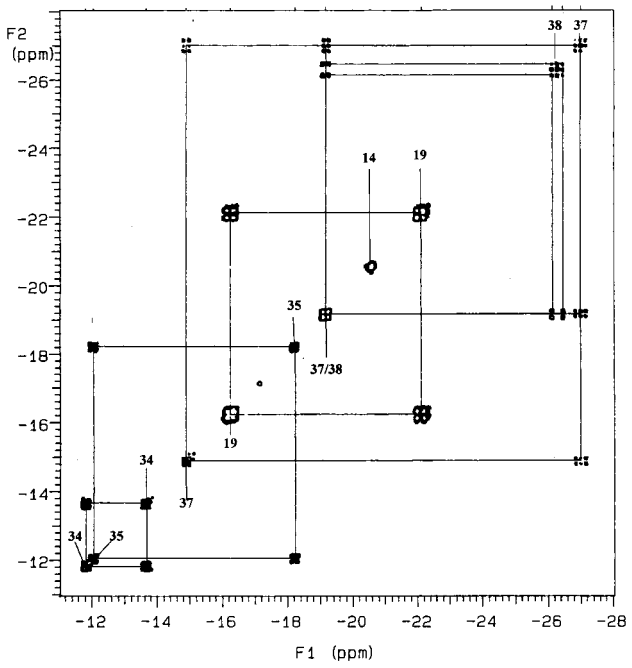

Figure 10. ^{31}P COSY spectrum of the products and intermediates during reaction of (*R*)-**11** and (*R*)-**15** at 47.5 °C, recorded at −50 °C, solvent $CDCl_3/C_6D_6$, [L] = 0.01 M.

Table 3. ^{31}P NMR Chemical Shifts and Coupling Constants of Dioxadiphosphetane and Trimeric Intermediates Leading to the Formation of Diphosphate (*R,R*)-**14** during Reaction at 47.5 °C, Recorded at −50 °C (See the Text for Explanation)

compd	δ (^{31}P NMR) (ppm)	δ (^{31}P NMR) (ppm)	δ (^{31}P NMR) (ppm)	J_{PP} (Hz)
34	−11.4	−13.73		18.2
35	−11.68	−18.22		21.0
36				
37	−14.92	−26.33	−19.22	22.4/22.4
38	−19.24	−25.90	−25.90	22.4/22.4

The responsible intermediates are built up of three connected phosphorus units, on the basis of the 2D ^{31}P COSY spectrum as well as the observed coupling constants and integration data. The doublet at δ −14.92 ppm is correlated to the double doublet at δ −26.33 ppm ($^2J_{PP}$ = 22.4 Hz). The latter shows a correlation with the signal resonating at δ −19.22 ppm ($^2J_{PP}$ = 22.4 Hz). It is clear that the phosphorus atom leading to the signal at δ −26.33 ppm is connected with two other, nonequivalent, phosphorus atoms that are not directly correlated themselves. The only possible explanation for this peculiar phenomenon is the coupling of three phosphorus-containing units into an intermediate noncyclic trimer. The use of oxygen-labeled (*R*)-**11** shows that the resonances at δ −26.33 ppm double, and the resonances residing at δ −14.92 ppm show complex behavior (the effects are unfortunately only observable in the early stages of the reaction). Oxygen labeling does not influence the other resonance, residing at δ −19.22 ppm. The chemical shift data together with the integration data, coupling constants, and the data obtained from the oxygen-labeling experiments indicate that the trimeric intermediate has structure **37** (Scheme 11). This compound contains three different phosphorus atoms and is formed from hydroxyphosphorinane (*R*)-**15**, which has attacked chlorophosphorinane (*R*)-**11**. Subsequently, this unit attacks another chlorophosphorinane (*R*)-**11**, yielding the trimer as suggested.

The other trimer **38** also contains three phosphorus atoms, although two of them appear to be "virtually" equal, resulting in a doublet at δ −19.24 ppm ($^2J_{PP}$ = 22.4 Hz) and an apparent triplet at δ −25.90 ppm. These resonances show two equal $^2J_{PP}$ couplings of 22.4 Hz and a measured intensity half the size of the resonance at δ −19.24 ppm. Although this structure contains a bisequatorially spanned phosphorinane ring system, which is assumed to be energetically unfavorable, this is the only possible structure which contains two equivalent phosphorinane ring systems and can still lead to the exclusive formation of (*R,R*)-**14** and no other products.

The use of ^{18}O-labeled (*R*)-**11** leads to the doubling of the signals at δ −25.90 ppm and to a partial doubling of the signal at δ −19.24 ppm, while a part of this signal remains unaffected (again, only in the early stages of this reaction). Obviously, hydroxyphosphorinane (*R*)-**15** reacted with 1 equiv of chlorophosphorinane (*R*)-**11** that reacted with another molecule of

Scheme 10. Formation of **14** via Dioxadiphosphetanes

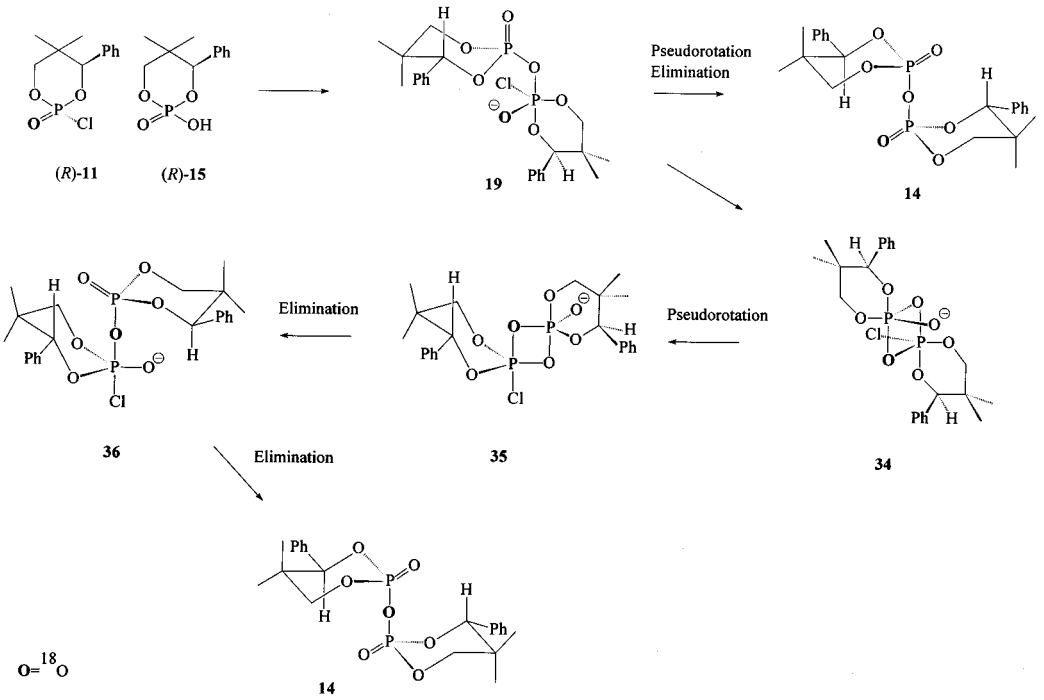

Scheme 11. Proposed Structures of Intermediates **37** and **38** (^{31}P NMR Chemical Shifts Indicated)

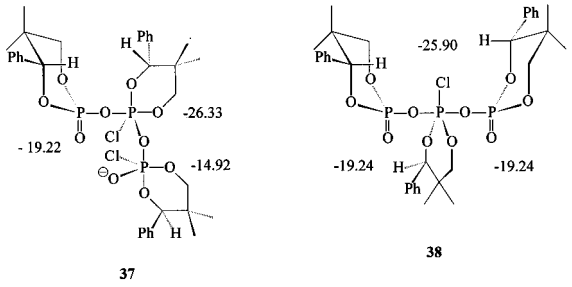

chlorophosphorinane (*R*)-**11**, yielding intermediate **38**. This is the elimination product of intermediate **37**. Intermediate **38** can only be transferred into (*R,R*)-**14** after another attack of a molecule of deprotonated hydroxyphosphorinane (*R*)-**15** has taken place. This would afford one molecule of (*R*)-**15** and one molecule of chlorophosphorinane (*R*)-**11**, together with one molecule of diphosphate (*R,R*)-**14** (Scheme 12).

Alternatively, chloride attack on **38** could result in one molecule of (*R*)-**11** and one molecule of diphosphate (*R,R*)-**14**, together with one chloride anion (Scheme 12). Furthermore, intermediate **37** can be converted either into **38** by chloride elimination or into diphosphate (*R,R*)-**14** by elimination of (*R*)-**11** and a chloride anion.

Unfortunately, it appeared impossible to generate the same types of intermediates by using one of the other hydroxyphosphorinanes or chlorophosphorinanes with substituted phenyl groups, or combinations of hydroxyphosphorinanes or chlorophosphorinanes, regardless of the reaction conditions employed.

It is clear that besides the *direct* route and the chloride attack, followed by the direct route, another reaction mechanism, involving trimeric structures, can also give rise to the formation of diphosphate (*R,R*)-**14**.

Conclusions

The unusual *minor* side reaction observed when reagent (*R*)-**11** or (*R*)-**17** is used for enantiomeric excess determination of

Scheme 12. Alternative Mechanism for the Formation of Diphosphate **14** from **37** and **38**

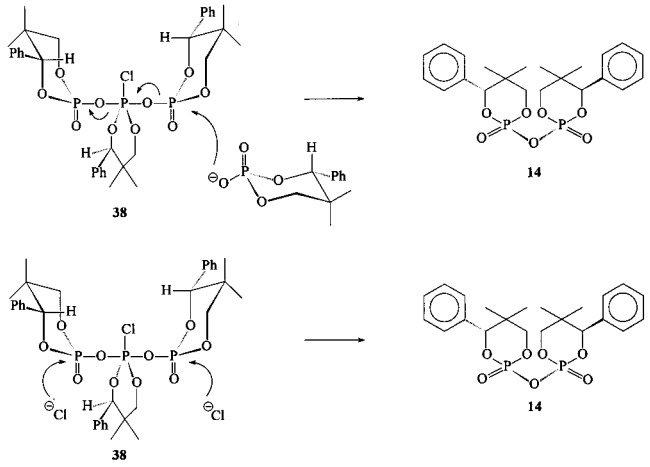

amines, alcohols, or amino acids provides a rich source of information concerning the formation of diphosphates in general. Although the side reaction does not influence the actual analyses, the appearance of side products gave rise to a more detailed investigation.

The products formed were characterized as diphosphate (*R,R*)-**14** and intermediates leading to its formation. Due to the conformational *locking* of the phenyl group in the equatorial position of the "phencyphos" building units, the pseudorotation intermediate products are blocked, and allow detection of intermediates using ^{1}H and, in particular, ^{31}P NMR techniques. On the basis of the data obtained from several NMR experiments, the use of ^{18}O-labeled chlorophosphorinane (*R*)-**11** and the stereochemical information from racemic and homochiral chlorophosphorinane **11** and hydroxyphosphorinane (*R*)-**15**, it was concluded that the nucleophilic displacement reaction proceeds with complete stereocontrol at the phosphorus center. An explanation can be given on the basis of a mechanism involving *phosphetane* intermediates (mechanism 1), as is depicted in Scheme 10. These results are in agreement with the

results using related *achiral* compounds, as reported by Zwierzak[3,4] and Cullis.[6,8] More important, however, is the fact that the results obtained by Cullis and Zwierzak are only based on the products obtained. Using the phencyphos derivatives, several intermediates can actually be observed using ^{1}H and ^{31}P NMR techniques.

Labeling experiments with ^{18}O-labeled (*R*)-**17**, and hence (*R*)-**11**, together with the use of racemic hydroxyphosphorinanes **15** and **28** as well as chlorophosphorinane **11** and **27**, made the complete structural assignment of the observed intermediates possible. Furthermore, the scrambling of the oxygen over all possible exocyclic oxygens in this system showed not only that a direct nucleophilic displacement reaction of hydrogen−phosphorinane **15** and chlorophosphorinane **11** occurred, but also that a second mechanism must operate.

The use of *mixed* phencyphos hydroxyphosphorinanes (**15** and **28**) and chlorophosphorinanes **11** and **27** showed that eliminated anionic chloride is able to act as a nucleophile, attacking the "mixed" diphosphate **32**. This yields combinations of chlorophosphorinanes and reaction intermediates, which were not apparent at the start of the reaction following mechanism 1 (Scheme 9), or could be formed during the reaction otherwise. These observations could provide another explanation for the scrambling of the ^{18}O-label over the different oxygen atoms in both products and intermediates.

Using 2D ^{31}P COSY NMR techniques, together with ^{18}O-labeling experiments, a third mechanism was found (Schemes 11 and 12). In this mechanism, acyclic trimeric phosphorus-containing intermediates **37** and **38** are formed, leading to the direct formation of diphosphate (*R,R*)-**14**, or to the formation of diphosphate (*R,R*)-**14** after the attack of a deprotonated hydroxyphosphorinane unit. This also results in complete scrambling of ^{18}O-labeled oxygens over all the exocyclic oxygens. Alternatively, chloride attack on the trimeric intermediates would give the described products. In this way, hydroxyphosphorinanes and chlorophosphorinanes bearing ^{18}O-labels are formed at the beginning of the reaction. These compounds can react further, and give rise to doubly or triply ^{18}O-labeled (*R,R*)-**14**.

Although probably all three mechanisms, involving (1) the formation of phosphetanes as proposed by Zwierzak[3,4] and Cullis and co-workers,[6] (2) chloride attack at the diphosphate formed, or (3) trimer formation followed by attack of deprotonated hydroxyphosphorinane or chlorophosphorinane, are not in disagreement with each other, the appearance of the last two routes has to the best of our knowledge never been proposed or observed previously.

It is remarkable that, although the reaction routes are rather complex and markedly different, the final product, diphosphate (*R,R*)-**14**, is always formed as the only enantiomerically pure product. This means that the reactions proceed with complete stereocontrol with regard to the phosphorus nucleus, regardless of the route followed.

Experimental Section

All operations were carried out using Schlenck-line techniques under an argon atmosphere. NMR measurements were performed in well-dried and sealed NMR tubes, using predried solvents under an argon atmosphere.

1D NMR spectra were taken at 30 °C (±0.1 °C), unless stated otherwise, using Varian temperature control units. ^{1}H and ^{13}C NMR (APT) spectra were recorded on Varian VXR-300, Unity-400 WB, and UnityPlus-500 spectrometers at 300, 400, and 500 Hz and 75.43, 100.57, and 125.72 MHz for proton and carbon, respectively. Chemical shifts are denoted in δ units (ppm) relative to the solvents and converted to the TMS scale. The splitting patterns are designated as follows: s (singlet), d (doublet), dd (double doublet), t (triplet), q (quartet), m (multiplet), and br (broad). Chemical shifts (ppm) are positive in the low-field direction.

^{1}H decoupled ^{31}P NMR spectra were recorded on Varian VXR-300 and Unity-400 WB spectrometers operating at 121.42 and 161.89 MHz, respectively. The chemical shifts are denoted either relative to $(NPCl_2)_3$ resonating at δ 19.91 ppm (for the solvents $CDCl_3$ and C_6D_6) or relative to phosphoric acid at δ 0 ppm (for the solvents D_2O, DMSO-d_6, and CD_3OD). T_1 relaxation times were calculated with the inversion−recovery method, using standard Varian microprograms. The $^{1}H-^{1}H$ and $^{31}P-^{31}P$ COSY, $^{1}H-^{1}H$ NOESY, and $^{1}H-^{1}H$ ROESY spectra were recorded at +50, 0, and −50 °C (±0.1 °C) using Varian Unity-400 WB and UnityPlus-500 spectrometers. The 2D spectra were collected as 2D hypercomplex data. After weighing with shifted sine-bell functions, the COSY[49] data were Fourier transformed in the absolute value mode while the NOESY[50] and ROESY[51] data were transformed in the phase-sensitive mode. Data processing was performed using standard Varian VnmrS/VnmrX software packages. The spectrometers operated in the Fourier transform mode using the ^{2}H resonance of the solvent as field-frequency lock.

The hydroxyphosphonates and phosphonate (*R*)-**17** were prepared according to literature procedures.[25,26] ^{18}O-labeled water (labeling degree around 85%, as established from the integration of the two signals in the ^{31}P NMR spectra) was kindly provided by the PET Center at the University Hospital of Groningen, The Netherlands. Diphosphate (*R,R*)-**14** was also prepared for comparison purposes according to the method described by Edmundson.[5]

(*R*)-2-Chloro-2-oxo-5,5-dimethyl-4-(*R*)-phenyl-1,3,2-dioxaphosphorinane [(*R*)-11]. Using the PCl_5 Method. (*R*)-Phencyphos (*R*)-**15** (40.0 g, 0.17 mol) was suspended in 250 mL of dry CH_2Cl_2. To this stirred suspension was added 40.0 g of PCl_5 (0.19 mol) over a 10 min period, while the temperature was kept below 10 °C. Subsequently, the mixture was stirred for 3 h at room temperature. The solution was concentrated to dryness and the residue dissolved in 250 mL of dry ether. Excess PCl_5 was removed by filtration and the filtrate stored at −20 °C for 7 days. After this period, small white needles were isolated and dried carefully in a vacuum at 35 °C for 2 h. Yield of (*R*)-**11**: 7.02 g (0.027 mol, 16%). Mp 156−158 °C. $[a]^{20}_D = -81.9°$ (*c* 0.5, $CHCl_3$). ^{1}H NMR ($CDCl_3$): δ 0.82 (s, 3H), 1.03 (s, 3H), 4.03 (dd, $^{2}J_{AB} = 9.0$ Hz, $^{3}J_{PH} = 30.0$ Hz, 1H), 4.18 (dd, $^{2}J_{AB} = 9.0$ Hz, $^{3}J_{PH} = 4.0$ Hz, 1H), 5.21 (d, $^{3}J_{PH} = 2.0$ Hz, 1H), 7.20−7.40 (m, 5H). ^{13}C NMR ($CDCl_3$): δ 17.14 (CH_3), 20.64 (CH_3), 36.36 (d, $^{3}J_{PC} = 4.6$ Hz, C), 79.51 (d, $^{2}J_{PC} = 8.1$ Hz, CH_2), 89.78 (d, $^{2}J_{PC} = 6.9$ Hz, CH), 127.16 (CH), 127.93 (CH), 128.86 (CH), 134.67 (C). ^{31}P NMR ($CDCl_3$): δ −4.49 ppm. Anal. Calcd for $C_{11}H_{14}O_3PCl$: C, 50.69; H, 5.41; P, 11.88; Cl, 13.60. Found: C, 50.34; H, 5.22; P, 11.48; Cl, 13.47. HRMS: calcd 260.037, found 260.037.

Using the $POCl_3$ Method. A solution of 8.0 g (0.052 mol) of $POCl_3$ in 500 mL of CH_2Cl_2 was cooled to −20 °C. To the stirred solution was slowly added a solution of 10.0 g (0.052 mol) of (*R*)-phencydiol (*R*)-**16** and Et_3N (12 mL) in 200 mL of CH_2Cl_2. After the addition was complete (30 min) another 12 mL of Et_3N in 50 mL of CH_2Cl_2 was added. The mixture was stirred for 5 h and concentrated and the residue dissolved in ethyl acetate. The solution was filtered and evaporated to dryness, and the residue was dissolved in ether and stored at −20 °C to allow the chlorophosphorinane (*R*)-**11** to crystallize. After 7 days, small white needles were collected and treated as described above. Yield: 3.81 g (0.0146 mol, 28%). Spectroscopic data were found to be identical compared to those of the material obtained by the PCl_5 method.

Using the CCl_4-Et_3N Method. To a cooled (0 °C) mixture of 5.0 g (0.022 mol) of cyclic (*S*)-hydrogen−phosphorinane (*S*)-**17** and 3.4 g

(49) Bax, A.; Freeman, R. *J. Magn. Reson.* **1981**, *44*, 542.

(50) Jeener, J.; Meier, B. H.; Bachmann, P.; Ernst, R. R. *J. Chem. Phys.* **1979**, *71*, 4546. Neuhaus, D.; Williamson, M. *The Nuclear Overhauser Effect in Structural and Conformational Analysis*; VCH Publishers: Cambridge, 1989.

(51) Bothner-By, A. A.; Stephens, R. L.; Lee, L.; Warren, C. D.; Jeanloz, R. W. *J. Am. Chem. Soc.* **1984**, *106*, 811.

Table 4. Crystallographic Data for Crystal Structure Determinations of **12**, **13**, and **27**

	12	**13**	**27**
		Crystal Data	
empirical formula	$C_{20}H_{25}O_4P$	$C_{19}H_{24}NO_3P$	$C_{11}H_{13}Cl_2O_3P$
molecular weight	360.37	345.36	295.08
cryst syst	orthorhombic	trigonal	orthorhombic
space group	$P2_12_12_1$ (no. 19)	$P3_1$ (no. 144)	$P2_12_12_1$ (no. 19)
a, Å	6.4799(10)	12.4170(12)	6.4383(10)
b, Å	17.165(2)		10.498(2)
c, Å	17.189(2)	10.912(2)	19.571(3)
V, Å^3	1911.9(4)	1457.0(3)	1322.8(4)
D_{calc}, g cm^{-3}	1.252	1.181	1.482
Z	4	3	4
F(000)	768	552	608
μ, cm^{-1}	1.6 [Mo Kα]	13.7 [Cu Kα]	6.0 [Mo Kα]
cryst color	colorless	colorless	colorless
cryst size, mm	0.18 × 0.45 × 1.1	0.05 × 0.05 × 0.70	0.15 × 0.15 × 0.25
		Data Collection	
T, K	295	295	150
θ_{min}, θ_{max}, deg	1.2, 25.0	4.1, 75.0	1.6, 27.5
θ_{min}, θ_{max} (unit cell), deg	5.03, 10.71	7.13, 21.40	2.0, 20.0
wavelength, Å	0.71073 [Mo Kα]	1.54184 [Cu Kα]	0.71073 [Mo Kα]
filter/monochr	Ni filter	Zr filter	graphite monochr
$\Delta\omega$, deg	0.66 + 0.35 tan θ	0.62 + 0.14 tan θ	
hor, ver aperture, mm	2.30, 4.00	3.93, 6.00	
mosaicity			0.348(1)
X−ray exposure, h	32	45	6
linear instability, %	<1	3	
data set	0:8, −22:0, −22:22	−15:15, −15:15, −13:13	−8:8, −13:13, −25:25
total no. of data	1966	5772	35198
total no. of unique data	1958	5742 [R_{int} = 0.0575]	3040 [R_{int} = 0.0769]
		Refinement	
no. of refined params	246	223	206
final $R1$[a]	0.0511 [1061 $I > 2\sigma(I)$]	0.0631 [2417 $I > 2\sigma(I)$]	0.0228 [2941 $I > 2\sigma(I)$]
final w$R2$[c]	0.1001	0.1678	0.0590
goodness of fit	0.923	0.983	1.059
w^{-1} [c]	$\sigma^2(F^2) + (0.0416P)^2$	$\sigma^2(F^2) + (0.0879P)^2$	$\sigma^2(F^2) + (0.0323P)^2 + 0.21P$
$(\Delta/\sigma)_{av}$, $(\Delta/\sigma)_{max}$	0.000, 0.000	0.001, 0.008	0.000, 0.001
min and max residuals density, e Å^{-3}	−0.22, 0.19	−0.18, 0.19	−0.32, 0.18

[a] $R1 = \sum||F_o| - |F_c||/\sum|F_o|$. [b] $wR2 = [\sum[w(F_o^2 - F_c^2)^2]/\sum[w(F_o^2)^2]]^{1/2}$. [c] $P = (\max(F_o^2,0) + 2F_c^2)/3$.

(0.022 mol) CCl_4 in 150 mL of dry benzene was added 5 mL of Et_3N over 15 min. Subsequently, the mixture was allowed to stir at room temperature for another hour. The mixture was concentrated to dryness and the residue dissolved in dry ethyl acetate, filtered, and concentrated again to dryness. The residue was dissolved in petroleum ether (60:40, 75 mL) and stored for 7 days at −20 °C. After this period, white needles were formed that were treated as described above. Yield: 5.45 g (0.021 mol, 95%). Spectroscopic data were found to be identical compared to those of the material obtained by the PCl_5 method.

(*R*)-2-Chloro-2-oxo-5,5-dimethyl-4-(*R*)-(2-chloro-1-phenyl)-1,3,2-dioxaphosphorinane [(*R*)-27]. ^{1}H NMR ($CDCl_3$): δ 0.94 (s, 3H), 1.22 (s, 3H), 4.11 (dd, $^2J_{AB}$ = 11.5 Hz, $^3J_{PH}$ = 31.3 Hz, 1H), 4.46 (dd, $^2J_{AB}$ = 11.5 Hz, $^3J_{PH}$ = 3.0 Hz, 1H), 5.95 (d, $^3J_{PH}$ = 3.1 Hz, 1H), 7.22−7.42 (m, 3H), 7.52−7.60 (m, 1H). ^{13}C NMR ($CDCl_3$): δ 17.27 (CH_3), 19.86 (CH_3), 37.19 (C), 79.36 (CH_2), 84.23 (CH), 126.36 (CH), 129.07 (CH), 129.81 (CH), 131.83 (C), 132.36 (C). ^{31}P NMR ($CDCl_3$): δ −2.29 ppm. For other spectroscopic data see Ten Hoeve and Wynberg.[25]

(*R*,*R*)-2,2′-Oxybis(5,5-dimethyl-4-(*R*)-phenyl-1,3,2-dioxaphosphorinan-2-one) [(*R*)-14]. White crystalline material. Mp 143−145 °C. ^{1}H NMR ($CDCl_3$): δ 1.81 (s, 6H), 1.05 (s, 6H), 4.01−4.20 (ddd, 2H), 4.62−4.79 (d, 2H), 5.43 (dd, 2H), 7.19−7.38 (m, 10H). ^{13}C NMR ($CDCl_3$): δ 16.99 (dd, CH_3), 20.49 (dd, CH_3), 45.43 (CH_2), 79.76 (dd, C), 89.29 (dd, CH), 127.16 (CH), 127.76 (dd, CH), 128.54 (CH), 134.49 (C). ^{31}P NMR ($CDCl_3$): δ −20.56 ppm. HRMS: calcd 466.131, found 466.131.

X-ray Crystal Structure Analyses of 12, 13, and 27. (*R*)-2-Chloro-2-oxo-5,5-dimethyl-4-(*R*)-phenyl-1,3,2-dioxaphosphorinane [(*S*)-27] was prepared as described above for (*S*)-**11** using the PCl_5 method and was crystallized several times from diethyl ether at −20 °C.

(*R*)-2-O-[2′-(*S*)-phenylpropanoyl]-2-oxo-5,5-dimethyl-4-(*R*)-phenyl-1,3,2-dioxaphosphorinane [(*S*,*R*)-12] was prepared as described previously and recrystallized several times from ethyl acetate/diethyl ether mixtures at −20 °C.

(*R*)-2-*N*-[2′-(*S*)-phenylethanoyl]-2-oxo-5,5-dimethyl-4-(*R*)-phenyl-1,3,2-dioxaphosphorinane [(*R*,*S*)-13] was prepared as described previously and recrystallized several times from ethyl acetate/diethyl ether mixtures at −20 °C.

Pertinent data for the structure determinations are collected in Table 4. Data for crystal structures **12** and **13** were collected on a Nonius CAD4-F diffractometer on a sealed tube ($\omega/2\theta$ scans). Data for structure determination of **27** were collected on a Nonius κ-CCD diffractometer on a rotating anode. Accurate unit-cell parameters and an orientation matrix were determined by least-squares fitting of the setting angles of 25 well-centered reflections (SET4)[52] for structures **12** and **13**. The unit-cell parameters for structure **27** were refined against the setting angles of 485 reflections. The unit-cell parameters were checked for the presence of higher lattice symmetry.[53] All structures were solved with direct methods using SHELSX86.[54] Refinement on F^2 was performed with SHELXL-92[55] (**12** and **13**) or SHELXL-97-2 (**27**).[56] The hydrogen atoms of **12** and **13** were included in the refinement on calculated positions riding on their carrier atoms, except for the amine

(52) de Boer, J. L.; Duisenberg, A. J. M. *Acta Crystallogr*. **1984**, *A40*, C-410.
(53) Spek, A. L. *J. Appl. Crystallogr*. **1988**, *21*, 578.
(54) Sheldrick, G. M. SHELXS86 Program for crystal structure determination, University of Göttingen, Germany, 1986.
(55) Sheldrick, G. M. SHELXL-92 Program for crystal structure refinement, Gamma test version, University of Göttingen, Germany, 1992.
(56) Sheldrick, G. M. SHELXL-97-2 Program for crystal structure refinement, University of Göttingen, Germany, 1997.

hydrogen of **13**, which was located on a difference Fourier map and freely refined. All hydrogen atoms of **27** were freely refined. The hydrogen atoms of **12** and **13** were refined with a fixed isotropic displacement parameter related to the value of the equivalent isotropic displacement parameter of their carrier atoms; the hydrogen displacement parameters of **27** were freely refined. The absolute configuration for all compounds was assigned in accordance with the known configuration of the asymmetric carbon atoms. For compound **27** a full Friedel-related data set was collected. A racemic twin refinement indicated 100% *S* configuration on C_3, after which the twin model was abandoned. The Flack *x* parameter[57] for the final refinement was −0.01(5). The *x* parameter for the alternative chirality amounted to 1.00(5), with wR2 = 0.0640 and R1 = 0.0245.

Neutral atom scattering factors and anomalous dispersion corrections were taken from the *International Tables for Crystallography*.[58] Geometrical calculations and illustrations were performed with PLATON;[59] all calculations were performed on a DEC Alpha 255 station.

(57) Flack, H. D. *Acta Crystallogr*. **1983**, *A39*, 876.

Acknowledgment. Mr. K. Dijkstra and Dr. G. Visser are gratefully acknowledged for their useful contributions. Part of this work was supported by the council for Chemical Sciences of The Netherlands Organization for Scientific Research (CW-NWO) and DSM Research (Geleen, The Netherlands) (A.L.S., W.J.J.S.).

Supporting Information Available: Further details of the structure determinations, including coordinates and thermal parameters, as an X-ray crystallographic file (CIF) and as scanned tables. This material is available free of charge via the Internet at http://pubs.acs.org.

JA992770K

(58) Wilson, A. J. C., Ed. *International Tables for Crystallography*; Kluwer Publishers: Dordrecht, The Netherlands, 1992; Vol. C.

(59) Spek, A. L. *Acta Crystallogr*. **1990**, *A46*, C-34.